

1115.5  
NACA/33

MAY 12 1947

ACR June 1939



3 1176 00073 1910

Copy 2

WTRL-343

NATIONAL ADVISORY COMMITTEE FOR AERONAUTICS

# WARTIME REPORT

ORIGINALLY ISSUED  
June 1939 as  
Advance Confidential Report

PRELIMINARY REPORT ON LAMINAR-FLOW AIRFOILS AND  
NEW METHODS ADOPTED FOR AIRFOIL AND  
BOUNDARY-LAYER INVESTIGATIONS

By Eastman N. Jacobs

Langley Memorial Aeronautical Laboratory  
Langley Field, Va.

# NACA

WASHINGTON

NACA WARTIME REPORTS are reprints of papers originally issued to provide rapid distribution of advance research results to an authorized group requiring them for the war effort. They were previously held under a security status but are now unclassified. Some of these reports were not technically edited. All have been reproduced without change in order to expedite general distribution.

L - 345

NACA LIBRARY  
LANGLEY MEMORIAL AERONAUTICAL  
LABORATORY  
Langley Field, Va.

PRELIMINARY REPORT ON LAMINAR-FLOW AIRFOILS AND  
NEW METHODS ADOPTED FOR AIRFOIL AND  
BOUNDARY-LAYER INVESTIGATIONS

By Eastman N. Jacobs

SUMMARY

Recent developments in airfoil-testing methods and fundamental air-flow investigations, as applied to airfoils at the N.A.C.A. laboratory, are discussed. Preliminary test results, obtained under conditions relatively free from stream turbulence and other disturbances, are presented. Suitable airfoils and airfoil-design principles were developed to take advantage of the unusually extensive laminar-boundary layers that may be maintained under the improved testing conditions.

For practical consideration, these preliminary results presented are of interest mainly in the lower Reynolds Number range below 6,000,000. Within this Reynolds Number range the new laminar-flow airfoils and the new airfoil-design principles may be expected to yield drag coefficients on actual wings of a markedly smaller order than those heretofore obtained. For example, drag coefficients as low as 0.0022 and profile  $L/D$  values as high as 290 were measured.

INTRODUCTION

During the past several years there has been a growing conviction that large drag reductions should be possible through the use on actual airfoils of the low-drag properties of laminar boundary layers. In the past, however, the turbulence present in most wind tunnels tended to so hasten transition, in the usual full-scale range of the Reynolds Number, that the extent of the laminar layer appeared so small that only slight drag reductions could be expected from the low-drag properties of the laminar layers.

More recently, however, tests such as those made in flight to study the occurrence of transition under conditions of small air-stream turbulence (references 1 and 2) suggested that transition might occur much later. Furthermore, tests made in tunnels having moderately low turbulence tended to show some drag reduction owing to the presence of laminar layers of appreciable extent on propeller sections in the lower Reynolds Number range (reference 3) and in the lower full-scale range for airfoils (reference 4). The results of tests (reference 5) in the air stream of the N.A.C.A. smoke tunnel, which is known to have vanishingly small turbulence, as well as some of G. I. Taylor's theoretical considerations, led the author to the conclusion (reference 6) that more extensive laminar boundary layers and consequently larger drag reductions even at much larger Reynolds Numbers might be possible with suitable turbulence-free conditions simulating closely the turbulence-free atmosphere frequently encountered in flight.

During this period, plans were started for suitable low-turbulence large Reynolds Number airfoil testing equipment. The first step was to eliminate the complications of three-dimensional flows, thus reducing the problem to the two-dimensional flow about an airfoil section. The new type of airfoil testing equipment was therefore referred to as a "two-dimensional flow tunnel." The proposed methods of investigating airfoils extending across a comparatively narrow test section were thus truly tests of the airfoil section. In order to reduce the turbulence to such a level that its effect on transition should tend to vanish, variations of the methods employed in the N.A.C.A. smoke tunnel were contemplated.

The next step was to verify the proposed methods of airfoil testing. A small model of the new equipment was considered, but in order to obtain conclusive results a tunnel sufficiently large to reach the lower range of flight Reynolds Numbers was agreed upon.

The first and most difficult problem with the new equipment was to reduce the turbulence to the desired level. The usual methods of measurement were not sufficiently sensitive. Recourse was therefore had to the direct comparison of actual transition effects on airfoils as observed in flight, in the new tunnel, and in other tunnels. Such comparisons indicated that the turbulence as affecting transition could be reduced below the level of other tun-

nels and, in most cases, below the level inferred from many of the flight tests. (Compare, for example, fig. 13 of reference 2. Values of Jones'  $N$  exceeding 6,500,000 have been obtained from some of the recent tests of airfoils in the new tunnel.) Such comparisons suggest that transition was hastened in flight by other disturbing effects. In the tunnel, disturbances such as those due to surface roughness were carefully avoided and vibration effects were probably unimportant, at least at the lower air speeds. It remains improbable, nevertheless, that the desired effective zero turbulence (vanishing effect on transition) has yet been attained. The turbulence level was considered sufficiently low, however, pending more reliable comparisons with flight, to justify the airfoil development and the transition work herein reported in preliminary form.

In many ways, the preliminary results of these investigations have proved illuminating. It appears that, under these conditions of vanishing turbulence, transition may be of a different character than in the usual tunnel. The laminar-boundary layers ahead of transition often accurately follow the laminar-boundary layer theory and appear to be free or nearly free from unsteadiness or fluctuations of the Dryden type. Thus the skin-friction drags produced by these laminar layers at the comparatively large Reynolds Numbers attainable with the new equipment are no greater than the values predicted by the laminar-boundary layer theory.

The experimental airfoil investigations covered in a preliminary form in this report, moreover, are believed to be the first showing large drag reductions practically realizable through the design of airfoil sections to benefit from very extensive laminar-boundary layers. When airfoils are so designed that laminar separation is avoided, and particularly when falling pressures in the downstream direction are provided over a considerable portion of both upper and lower surfaces, laminar-boundary layers may be maintained up to Reynolds Numbers of 6,000,000 or more if sufficient care is exercised to eliminate disturbances from air-stream turbulence, surface roughness, and vibration. Such methods are shown to yield, within this relatively low Reynolds Number range, unusual drag reductions.

## DERIVATION OF AIRFOILS

The part of the investigation that resulted in the development of the new sections is best described by giving a brief chronological account of the work. Many associates contributed to the project, in particular, Pinkerton, von Doenhoff, Abbott, Stack, Robinson, Allen, Bicknell, and Miss Alice Rudeen, who made many of the pressure-distribution calculations. Their general assistance and contributions are acknowledged here for brevity in lieu of definite references to the detailed parts contributed by each.

The project was first undertaken as the result of reasoning like that presented in reference 6, which suggested possible late transitions in the presence of favorable pressure variations. Airfoil shapes were therefore sought having the minimum pressure on both surfaces well back. Trial shapes were used and results were checked by means of calculations according to Theodorsen's method of reference 7. Pinkerton, in particular, was successful in finding a shape (fig. 2) that was considered reasonably satisfactory for preliminary tests, although not as the basis of a family. Models having this section were constructed for tests in the variable-density tunnel and in the new tunnel.

Some doubt was expressed as to possible drag reductions, owing to the severity of the trailing-edge shape. The development of a suitable family was therefore not stressed, pending the completion of the new tunnel and the tests of this first section. In connection with Stack's project on propeller sections for high speeds, however, a special mean-line shape was derived by von Doenhoff and the author from thin airfoil theory to give a uniform chord-load distribution. When pressure-distribution calculations became available for some propeller sections having this mean line, it was apparent that its use, through adding a small constant velocity increment to the upper surface and deducting an equal increment from the lower surface, tended to leave both surface pressure distributions substantially unaltered. Hence it became necessary only to develop suitable thickness distributions for symmetrical airfoils giving the desired surface pressure variations.

In the meantime, the new airfoil testing equipment had been completed, and the first new airfoil (fig. 2) was test-

ed in June 1938. In comparison with an N.A.C.A. 0012 airfoil, tested under the same conditions, the new airfoil showed very extensive laminar-boundary layers, as expected, and the unusually low minimum drag coefficient of 0.0030. Comparative tests of the same airfoil in the variable-density tunnel, however, failed to show unusually low drag coefficients. Two very important conclusions therefore resulted from these preliminary tests. First, it is feasible to realize large drag reductions by designing airfoils to promote extensive laminar-boundary layers, even if such designs lead to an abnormally abrupt fairing in the trailing-edge region of the airfoil. Second, such airfoils must be investigated under conditions approaching freedom from turbulence.

A development program for this new airfoil type was therefore begun at once. The outstanding objectives of the investigation were to determine a limiting extent of the backward movement of the minimum pressure point on the airfoil surface and to investigate, in particular, various degrees of favorable pressure gradient in the forward or laminar region. Suitable thickness distributions (symmetrical airfoils) were therefore sought; and, to save time, these shapes were to be combined with only one mean camber selected to give the desired pressure distribution at  $c_l = 0.2$ , a reasonable high-speed or cruising lift coefficient.

The desired symmetrical airfoils were based on ones for which calculations had been made in connection with the high-speed airfoil investigations. One worked out by Robinson, through the process of pressure calculations following small empirical changes made to produce a nearly uniform pressure along the surface from a point near the leading edge to the 0.7c station was considered satisfactory as a member of the family having zero pressure gradient and was therefore designated N.A.C.A. 07.

Another airfoil, herein designated N.A.C.A. 16, was taken as a base for the next family, having favorable pressure gradients over the forward part of the profile. This base section may be considered the extension of the family of reference 3 that would therein have been given the number N.A.C.A. 0009-45; and may be accordingly derived.

Other airfoils of the same series were then derived to investigate the effects of a progressive backward movement

of the minimum pressure point. A compressing function was applied to the tail portion of the airfoil the function being so chosen as to leave the airfoil unaltered at maximum thickness where the two parts join. The function is given by

$$x' - 0.5 = \frac{1}{2k} \ln \{1 + k (2x-1)\} \quad (x \geq 0.5)$$

where  $x$  represents the original station for the airfoil of unit chord, and  $x'$  represents the new station. The resulting airfoil was subsequently stretched uniformly back to its normal chord length, the final result being a backward movement of the maximum thickness station. Pressure calculations for this group of airfoils having various positions of the maximum thickness indicated that such a series should be satisfactory. The members of this family of airfoils therefore received designation numbers as follows:

N.A.C.A. designation	16	18	19
Position of maximum thickness	0.5c	0.6c	0.7c
Approximate position of minimum pressure	0.6c	0.8c	0.9c
Leading-edge radius index (reference 3)	4	3	3

Thus the number 16 suggests the form of the thickness distribution and the complete designation number N.A.C.A. 16-209 for example, is formed by adding three more digits after the dash. The first digit increases with camber and refers to the lift coefficient, 0.2 in this case, for which the airfoil is designed. The last two digits refer to the thickness, 0.09c, in this example.

Finally, the test results for these airfoils and particularly for the modifications investigated with cusp-type extensions at the trailing edge to relieve the severity of the flow conditions in this vicinity, led to the development of a second series designated 27. This modified series, designated by the first digit 2, is much like the first, but the thickness distribution is modified to

produce a tendency toward a cusp-type tail. The mean line is also modified slightly near the trailing edge so that the lift-load distribution instead of being constant along the entire chord is constant only over the forward 80 percent and then tapers off progressively toward zero at the tail. This mean-line modification was considered desirable further to relieve the severity of the adverse pressure gradients in the turbulent-boundary-layer region near the trailing edge. This modified mean line was also used with some of the airfoils of the first series. The airfoil profiles included in this investigation are shown in figure 3.

### AIRFOIL ORDINATES

The airfoil ordinates may be derived by combining the camber and the thickness forms in the usual way, as explained in reference 8. The mean-line form may be found from the following general expression, worked out by Pinkerton and Allen:

$$\begin{aligned}
 y_c &= \frac{c_l}{2\pi(a+b)} \left[ \frac{1}{b-a} \left\{ \frac{1}{2} (a-x)^2 \ln |a-x| - \right. \right. \\
 &\quad \left. - \frac{1}{2} (b-x)^2 \ln |b-x| + \frac{1}{4} (b-x)^2 - \frac{1}{4} (a-x)^2 \right\} - \\
 &\quad \left. - x \ln x + g - hx \right] \\
 g &= - \frac{1}{b-a} \left\{ a^2 \left[ \frac{1}{2} \ln a - \frac{1}{4} \right] - b^2 \left[ \frac{1}{2} \ln b - \frac{1}{4} \right] \right\} \\
 h &= \frac{1}{b-a} \left\{ \frac{1}{2} (1-a)^2 \ln(1-a) - \frac{1}{2} (1-b)^2 \ln(1-b) + \right. \\
 &\quad \left. + \frac{1}{4} (1-b)^2 - \frac{1}{4} (1-a)^2 \right\} + g
 \end{aligned}$$

where the chord is unity and the load is uniform from the leading edge ( $x = 0$ ) to the chordwise position  $x = a$ , then tapers off uniformly to zero at  $x = b$ , and remains zero from this point to the trailing edge at  $x = 1$ . For the N.A.C.A. 27-215 airfoil with 0.5c trailing-edge extension,  $a = \frac{1.6}{3}$  and  $b = \frac{2}{3}$ . For the usual 27 group of airfoils,  $a = 0.8$ ,  $b = 1$ , and two other airfoils desig-

nated N.A.C.A. 07, 8-209 and 16, 8-215 have this same mean line. For the rest of the airfoils having the uniform-load mean line,  $a=b=1$ , and the expression for the mean line reduces to the simple form originally derived by von Doenhoff and the author:

$$y_c = - \frac{c_l}{4\pi} \left[ (1-x) \ln (1-x) + x \ln x \right]$$

$$\frac{dy_c}{dx} = \frac{c_l}{4\pi} \left[ \ln (1-x) - \ln x \right]$$

The value indicated by  $c_l$  is the "ideal" lift coefficient for which the airfoil is designed, 0.2 for most of the present sections. All the mean-line ordinates and slopes at standard stations are given in table I.

Ordinates for the thickness forms (symmetrical airfoils of the one maximum thickness 0.12c) are given in table II. Various airfoils of the present families may thus be derived by combinations of suitable camber and thickness forms. The method, now employed by some manufacturers, of laying out full scale the thickness ordinates perpendicular to the mean line at the standard stations, is definitely recommended for practical users of airfoils of these new families.

#### TEST METHODS

The airfoil models tested were of 3-foot span and usually of 5-foot chord. (See fig. 1.) They were of wood carefully machined to accurately laid-out and faired templates. During the investigation the matter of surface finish received much attention. Slight waviness or roughness was found to hasten transition so that during the earlier tests, the lacquer surface finish was progressively improved by sanding and filling to reduce any unfairness and small-scale roughness.

The first model was built by attaching a cover to a wooden frame but the slight tendency toward dimpling at the points of attachment gave marked adverse effects on transition. In fact, it appears that no perceptible three-dimensional dimples of this type can be tolerated. Such composite methods of construction were therefore abandoned.

No additional gain in surface smoothness on transition was realized, however, beyond that obtained by the use of 400 water cloth, working in the direction of the air flow to remove all appearances of slight depressions or elevations, although some slight gain may appear from polishing the extreme nose portion of the airfoil where the boundary layer is very thin. A surface R.M.S. roughness reading of 10 millionths of an inch was obtained from a "profilometer" measurement on a typical model. A better qualitative impression of the surface condition may perhaps be had from the estimate that the finish did not need to be as smooth as a high-grade automobile finish.

No attempt will be made to describe the tunnel and the detailed testing methods in this preliminary report. The air-flow uniformity in respect to both turbulence and distribution throughout the test section is such that departures from the desired conditions are extremely difficult to determine.

The investigations were generally of an exploratory nature and followed no routine procedure. It was at first planned to use a balance to obtain some force measurements, but it later appeared that air-flow and wake-survey methods were giving all the information required for the preliminary tests. Consequently, a tunnel balance has not been installed.

The usual testing procedure was first to estimate the drag from the integral of total-pressure-defect measurements in the wake for several angles of attack near that of minimum drag to find the angle corresponding to the most favorable flow conditions on the airfoil. Later an "integrating" manometer connected with a survey "rake" was employed. This arrangement gave a direct indication of the drag by the depression in the general liquid level in the unaffected tubes, which are associated with the rake tubes that lie outside the wake. The method should be apparent from figure 4, which shows the wake from 0.1-inch-diameter tubes spaced on 0.2-inch centers and located in the wake 0.4c behind the trailing edge of the 5-foot-chord models. The wake in figure 4(a) is from an N.A.C.A. 0012 airfoil at zero lift and the wake in figure 4(b) is from one of the low-drag airfoils at approximately its design lift. The separate tubes at the left indicate the tunnel dynamic pressure and the wake static pressure.

The airfoil drags were thus estimated over a range of

angles and Reynolds Numbers to define the region to be covered by boundary-layer surveys and pressure-distribution determinations. These determinations by means of a "mouse" somewhat like those described in reference 2 (see also fig. 1) were usually restricted to the angle of most favorable flow conditions. The principal objectives were to study the boundary layers and the transition points as a function of the Reynolds Number, to compare the experimental and theoretical pressure distributions, to investigate possible regions of separation (both laminar and turbulent) and their effects, and finally to determine the optimum lift coefficient. Some of these determinations are further discussed when the results are presented.

Finally, some of the airfoils were tested in the variable-density tunnel in order to indicate the usual over-all airfoil characteristics and also the drag characteristics for extremely large Reynolds Numbers or other cases where transition effects tend to be suppressed. These results may also be employed to estimate the maximum lift to be expected in flight. The tests therefore include some in which split flaps are applied to the sections.

## RESULTS

No attempt has been made to present these preliminary results in a complete or final form. Only the more significant results are included and no corrections have been applied, except to the results from the variable-density tunnel. The  $c_d$  values given are simply the integrals from the total-pressure-defect measurements. A small correction will eventually be applied for the survey-tube size (effective centers not the geometric centers). Perhaps an improved approximation to the true drag results would have been obtained by the use of the Jones formula, but no corrections of this type are being made pending the completion of an investigation now in progress to determine the correct methods of drag measurement by the wake-survey method in a closed tunnel. In general, it appears that the more exact methods will always result in corrections that will reduce the drag values presented. These corrections may, in some cases, be of the order of 15 percent.

Tunnel-wall corrections should also be applied to the results of pressure measurements on the airfoil surfaces. In the future, this difficulty will probably be avoided by

testing an airfoil somewhat thinner than the section it is to represent. For example, the surface pressure drop near the minimum-pressure point on an airfoil of 5-foot chord with a 15-percent-thick section in the tunnel is about 8 percent more than it would be in free air. Such restriction effects, of course, influence the lift results from the pressure determinations, although this error has been approximately removed by correction from some of the results for comparison with those from the variable-density tunnel and presented in figures 28 to 33. A small velocity-measurement error, of the type that has sometimes been erroneously referred to as "blocking," may also be present tending further to reduce the coefficient values.

Transition was judged from observations of impact pressures from the inner mouse tube, which rested with its flattened lower wall against the wing surface. The effective height of the tube was usually about 0.008 inch. The velocity indicated by the difference between this impact pressure and the static pressure from the mouse static tube thus indicated the surface velocity gradient and consequently the local skin friction. Transition was judged as the beginning of a sudden and marked increase in this velocity as the tunnel speed was gradually increased to move the transition point across the wing-surface station under observation.

Later, an improved method that gave more precise results was adopted. The function  $\frac{(q_s)^{1/3}}{\sqrt{q}}$ , where  $q_s$  is the dynamic pressure indicated by the surface tube and  $q$  is the stream dynamic pressure, was plotted against  $\sqrt{q}$ . This procedure is substantially the equivalent of plotting against the Reynolds Number  $R$  a function of the surface velocity gradient:

$$\frac{\frac{d U_s / U_o}{d y_s / c}}{\sqrt{R}}$$

which tends to remain independent of the Reynolds Number as long as the surface tube remains relatively close to the surface in a truly laminar layer. Figure 5 shows the method applied to the determination of three transition

points on the N.A.C.A. 27-212. It will be noted that the function remains constant indicating a truly laminar layer in the low-speed range and then rises abruptly in the transition region. The transition points were taken as the positions indicated by the arrows in figure 5 at the knee of each curve.

The condition of the boundary layer just prior to transition was investigated by the hot-wire method to study in greater detail the nature of transition, and to find an explanation for the tendency of the transition function to rise slightly before the appearance of marked transition effects. A fine hot wire was used with a high-gain d.c. amplifier and a cathode-ray oscilloscope. The results obtained, some of which are indicated in figure 5, are rather significant. Well ahead of the transition point the laminar-boundary layer was remarkably steady and appeared to be free, or nearly free, from unsteadiness or fluctuations of the Dryden type. Perhaps such steady laminar layers should have been expected under the test conditions of very low turbulence in the new tunnel, particularly after it had been demonstrated that the experimental and theoretical boundary layers agreed excellently, both with respect to total layer thickness and the velocity profile within the layer, but Dryden (reference 9) had found from experiments that some layers may become markedly unsteady while, at the same time, retaining laminar properties, at least much more nearly laminar than turbulent. The oscilloscope showed, however, a quite different behavior as the Reynolds Number was increased to bring about transition. Instead of fluctuations in the laminar layer, the observations indicated momentary transitions to skin-friction intensities comparable with those of a fully developed turbulent layer but of extremely short duration, perhaps less than 0.01 second and at first occurring only once every several seconds. These very short bursts of turbulence were much too fast to appear in the over-damped mouse measurements, which indicated only a mean result. The reason for the early gradual rise of the transition function is thus apparent. The total time duration of the turbulent type of flow was of the order of 1 percent when the "transition point" indicated by the arrow at  $R = 6,000,000$  in figure 5 was reached. As the Reynolds Number was further increased, the frequency, and also the duration, of each of the turbulent bursts increased so that the relative total time in this condition increased as indicated by the percentage values given opposite the points in figure 5.

Pressure-distribution results, both theoretical and experimental, when extensive mouse static-pressure observations were made, are presented together in figures 6 to 21. In some cases, the theoretical pressures were obtained directly from calculations by Theodorsen's method (reference 7) and, in others, by Allen's method (reference 10) of velocity-increment addition to the velocities about the basic symmetrical section to allow for the lift-load distribution. This method is very simple and may be readily applied to the prediction of pressure distributions and critical speeds for other derived airfoils of the new families. For such purposes, the theoretical basic pressure distributions for the symmetrical sections are given in figure 22 and in tables III to VII.

Certain additional important data are also included in figures 6 to 21, in addition to the arrows indicating the measured transition-point positions, and the corresponding wing Reynolds Numbers indicated in millions near each arrow. Separation of the flow is also indicated as judged from the mouse measurements. Included also are the angle of attack, the corresponding measured minimum drag coefficient, and the Reynolds Number at which it occurred. The theoretical compressibility-bubble speeds, expressed as the ratio  $M_c$  of the critical speed to the speed of sound obtained both from the measured and the theoretical peak negative pressure coefficients by the method of reference 11, are also included in each figure.

Some other experimental data are presented with the discussion. Data dealing with further details of scale-effect calculations, skin-friction distribution, and boundary-layer studies in comparison with theory, the analysis of the transition data, the extension of these airfoil developments to higher Reynolds Numbers and speeds, studies of the relative tunnel turbulence, and check tests in other tunnels and in flight will be separately presented and discussed by various authors in subsequent papers.

## DISCUSSION

### Best Airfoil, the Optimum Reynolds Number Range

This discussion will first consider the experimental data on the various airfoil forms almost without regard to the Reynolds Number, considering mainly the minimum-drag

results in the range where the gains from extensive laminar flows were largest. Applications at higher Reynolds Numbers will be considered later. The emphasis on the minimum-drag results may appear inconsistent with earlier N.A.C.A. airfoil reports, but several factors have altered the point of view. A commendable trend has begun, led particularly by the Army Air Corps, away from an arbitrary landing-speed requirement that tends to fix the wing area in relation to  $C_{Lmax}$ . Changes in  $C_{Lmax}$  therefore no

longer necessarily produce corresponding changes in minimum wing drag through the process of forcing a change of wing area. High maximum lift coefficients, moreover, were often associated with large and abrupt lift losses beyond the maximum, a combination of perhaps less than no value except through the possibility of thus circumventing the arbitrary landing-speed requirements to affect area and drag reductions. Finally, the drag reductions possible through the realization of extensive laminar layers are relatively so large that  $C_{Lmax}$  variations tend to become

relatively unimportant between airfoils of slightly different shape, particularly when used with a high-lift device, as in figure 31, for example

The data should thus be considered first in relation to the more important factors affecting the minimum drag. As pointed out earlier, one of the objects of the investigation was to determine the limiting extent of the favorable pressure, or laminar flow run over the forward part of the airfoil and also the effects of variations in the degree of the pressure gradient within this range. As regards the limiting extent of the laminar layer, the drag results (figs. 23 to 27) show that it tends to increase as the airfoil thickness decreases. The lowest drag coefficient obtained was 0.0022 with the N.A.C.A. 18-204 section at a Reynolds Number of approximately 4,000,000. Figure 6 indicates that the extent of the laminar run was then more than 0.80c. The determinations indicated that this run could not be greatly increased. If an increase was attempted through a reduction of the Reynolds Number, wake fluctuations and drag increases were encountered. The adverse effects were evidently associated with transition occurring momentarily so far behind laminar separation that an incomplete closing in of the turbulent layer with consequent pressure drag was encountered. (See reference 12.) On the other hand, adverse effects also appeared when a further backward shift of transition was attempted through a backward movement of the minimum pressure point, as in

changing to the N.A.C.A. 19-204 section (fig. 7). The minimum drag coefficient obtained was 0.0029; this value indicates that such an extreme backward movement of the minimum-pressure point results in too blunt a trailing edge even for a 4-percent-thick airfoil. The pressure recovery and adverse gradients are evidently too severe to be overcome even by the most favorably situated turbulent layer.

Turning now to the 9-percent-thick airfoils (fig. 24), the 18 series is still found to have the lowest drag coefficient (0.0026), but the minimum now occurs at a higher Reynolds Number. This change may be attributed partly to a lower boundary-layer Reynolds Number  $R_\delta$  associated with the increasing airfoil thickness because of the resulting increased favorable pressure gradients over the laminar portion of the surface. Thus, if transition tends to occur at a given  $R_\delta$ , the given value will be reached at a higher  $R$  on the thicker wing. It is noteworthy also that the drag of the N.A.C.A. 27-209 airfoil reaches nearly as low a value and shows a considerably less marked rise at the higher Reynolds Numbers than the 18 airfoil. In fact, the cusp-type trailing edge was added to the 18 airfoil (fig. 10) in an attempt to reduce the severity of the trailing-edge conditions. The wake surveys and the surface-pressure determinations on this airfoil without the cusp were so erratic that the cusp was considered almost necessary to establish the circulation and lift so that accurate measurements could be made.

A consideration of the pressure diagram in figure 10 suggests another reason for the use of the cusp. With blunt trailing edges like those of the 18 series, a marked pressure drag may be associated with the failure of the actual surface pressures to rise toward the stagnation pressure at the trailing edge as the theory indicates they should when the form drag is zero. As shown by figure 10, the theory does not require for the cusp tail this unattainable type of pressure rise.

Associated poor pressure recoveries and marked form drags for the blunt airfoil are apparent in the results, particularly at Reynolds Numbers higher than that for minimum drag. Here the conditions in the turbulent layer become progressively less favorable for a pressure recovery as the transition point moves forward on the airfoil. The increased turbulent skin friction occurring ahead of the minimum pressure point thickens the turbulent layer at the

*with 9% t/c  
that was added acc.  
the b.l. stayed low  
at higher Reynolds  
numbers where  
thinner b.l. was*

beginning of the pressure recovery and hence makes the given adverse gradient relatively more severe. Under extreme conditions, turbulent separation may be expected.

Such considerations led to the development of the N.A.C.A. 27 series (fig. 11) which was designed to relieve the severity of the flow conditions in the pressure-recovery region behind the minimum pressure point. The expected reduction in drag at Reynolds Numbers above that for the minimum is shown in figure 25 and more particularly for the 12-percent-thick section in figure 26. The marked favorable result is not indicated for the N.A.C.A. 27-215 section (fig. 27), but the ordinates for the 27 series were revised between the time the 15 airfoil and the other airfoils were constructed. The ordinates of the airfoil that was tested are not now considered satisfactory as a member of the 27 family. The test results, although included, should therefore be discounted.

Another unanticipated result of changing from the 18 to the 27 series was the shift of the minimum drag to lower Reynolds Numbers. The same result is again indicated in figure 25 in changing the minimum pressure farther forward from 0.7c to 0.6c in going from the 27 to the 16 series. The opposite shift of the minimum drag to higher Reynolds Numbers was expected owing to the lower local Reynolds Number at the minimum pressure station at a given wing Reynolds Number. The explanation is that minimum drag with these airfoils does not occur when transition is near the minimum pressure point, or even forward of the laminar-separation point. (See figs. 12 and 18.) These experimental data do not conflict with the laminar-separation theory (reference 13), which places the laminar separation point very near the minimum pressure point after the layer has become thickened by its long run over the forward portion of the airfoil. When the minimum pressure point is not well back, minimum drag occurs at a Reynolds Number so low that moderately extensive laminar separation is actually present. The transition occurs soon enough to close in and permit the pressure recovery but not soon enough at minimum drag to produce excessive turbulent skin frictions. In the separated or adverse pressure range, however, this transition tends to occur at a reduced Reynolds Number.

Figure 25 also throws some light on the question of how steep the favorable pressure gradient should be over the forward part of the airfoil. A comparison of the

N.A.C.A. 07-209 and the N.A.C.A. 27-209 airfoils shows a higher minimum drag and an earlier rise with increasing Reynolds Number for the airfoil with the flat pressure distribution.

A tentative explanation can be given as the result of further fundamental boundary layer and transition studies not included in this report. The difficulty with the flat pressure distribution is not primarily that transition necessarily occurs at a much smaller value of  $R_\delta$  in the absence of a favorable pressure field, although there may be some slight tendency in this direction, but that very small disturbances such as slight imperfections in the model, slight departures from the design angle of attack, or slight flow fluctuations may produce regions of local adverse pressure gradient. This condition tends to produce regions of excessive boundary-layer thickness (or even local separation), which tend to grow three dimensionally in the absence of a favorable pressure gradient impelling the low-energy air along in the normal flow direction. Hence, excessive values of  $R_\delta$  may appear locally leading, in turn, to a premature transition. The optimum magnitude of the favorable pressure gradient for these airfoils therefore becomes largely a matter of practical compromise. Small gradients require extreme care in the elimination of disturbances, whereas large gradients cause excessive skin friction, excessive form drag due to the more severe pressure recoveries, and low critical speeds due to the excessive peak negative pressures.

### Applications

It thus appears that, within the Reynolds Number range considered, the N.A.C.A. 27 series represents a reasonable approximation to the best compromise. The lift at which the minimum drag occurs may be varied at liberty to meet particular design requirements. The extent to which the optimum lift may be increased is suggested by the results for the N.A.C.A. 27-2012 in figure 16. This airfoil was designed for an optimum lift coefficient of 2.0. Such an extreme procedure probably pushes the present design principles too far, but high-lift airfoils of this type may find some application. The ultimate performance of an airfoil section for application such as long-range airplanes, gliders designed for small gliding angles, blower and propeller blades, guide vanes, etc., is measured by the maximum profile  $L/D$  for the section. With these new

airfoil-design principles, low-drag coefficients may be attained at rather high lift coefficients. With the older type of flapped airfoil, for example, the pressure recovery realizable over the upper surface of the flap was restricted by the excessive thickness of the turbulent layer in this vicinity. Owing to the possibility of maintaining laminar flows over the forward portion of the new airfoils, the turbulent layer at the after part of the airfoil may be relatively thin with the result that relatively abrupt pressure recoveries are attainable. Although the boundary-layer studies on the N.A.C.A. 27-2012 indicated that the lift in this case had probably been pushed too high, a maximum profile  $L/D$  of over 290 was attained. For airfoils similarly designed but with slightly lower optimum lifts, the turbulent separation that occurs near the trailing edge may be sufficiently reduced to produce even higher  $L/D$  ratios.

By a suitable choice of the camber to give the desired optimum lift, the lift range of low drag (figs. 28 to 32) will be sufficient for many practical applications. Outside the low-drag range, the variable-density tunnel results suggest that the airfoil drag will not be excessive. The results presented herein are applicable only within the lower Reynolds Number range and therefore appear most naturally suited for application to small aircraft and gliders. It should not be overlooked that they may have much wider application to special designs in which it is feasible by reduction of wing chord or density at high altitudes to achieve the proper Reynolds Number. In application to airplane wing design the camber will probably be selected so that the optimum lift will occur near the cruising speed. An airfoil somewhere between the N.A.C.A. 27-112 and N.A.C.A. 27-512 will thus probably be employed. The advantage of the new sections will then appear through increased cruising speeds and in more economical operation within this speed range.

It should be emphasized, however, that the gains will not be marked unless suitable applications are selected. It may be desirable to employ unusually large aspect ratios in order to reduce the induced drag and to reduce the chord sufficiently to obtain a suitably low Reynolds Number. The wing surface must, of course, be fair and smooth over the forward 80 percent. Vibration should be avoided and, in all probability, the propeller slipstream on the wing must be eliminated. Pusher propellers are therefore to be recommended pending an experimental demonstration that the disturbing effects of the tractor propeller can be tolerated. Disturbances arising forward of the wing along the fuselage will affect only small portions of the wing ad-

jacent to the fuselage. Only that part of the wing inside a line extending from a point at the leading edge just outside the fuselage-boundary layer backward toward the trailing edge and outward with the flow direction at an angle probably less than  $8^\circ$  need necessarily be subjected to the usual high turbulent skin friction.

Most important of all in any application, however, is the reduction of fuselage, tail-surface, and parasite drags to a reasonable minimum. High parasite drags may easily mask any marked gain from a large reduction in wing-section drag. One private-owner type of airplane tested in the N.A.C.A. full-scale tunnel showed for example, a drag coefficient of approximately 0.0600. A reduction of wing drag from 0.0080 to 0.0030 would consequently have reduced the over all drag of the airplane only in the ratio 55/60. The resulting speed increase would thus represent an almost inappreciable gain. On the other hand, if the airplane to which the new wing is applied is so clean that the wing-profile drag represents a large part of the entire drag, the performance gains will be very large. The higher speeds attainable, in turn, reduce the induced power, and often improve the propeller efficiency. Particularly in bucking a head wind, the time saving and the economy expressed in miles per gallon, a matter of vital importance to the private flyer, should thus be improved to a very marked extent by the application of the new wing sections.

#### Applications at Reynolds Numbers Above the Optimum

Little will be said regarding the application of these data at the higher Reynolds Numbers because further investigations outside the scope of this report are now in progress to develop methods of maintaining these same low-drag properties at very high Reynolds Numbers. It appears, however, that comparatively small gains of this same type may be readily realized at the higher Reynolds Numbers by maintaining the laminar layers over only a comparatively small portion of the forward part of the airfoil. In fact, full-scale tunnel tests of the N.A.C.A. 23012 airfoil (reference 4), and of the N.A.C.A. symmetrical airfoils (reference 14), as well as tests of the N.A.C.A. 23012 airfoil to study roughness effects in the 8-foot high-speed tunnel, indicated that some gains of this type would be possible on existing airplanes if sufficient attention were given to the surface condition on the forward part of the wing.

Actually the gains might be noticeably larger in flight owing to tunnel-turbulence effects present in the test results. On the other hand, these types of airfoil are inherently unsuited to the desired flow conditions, except possibly at extremely large Reynolds Numbers. The "additional" type of lift distribution associated with the symmetrical airfoil, for example, causes a minimum-pressure peak to occur very near the leading edge on the upper surface. (See references 15 and 10.) This condition always tends to lead to premature laminar separation or transition.

An obvious improvement in the medium Reynolds Number range is possible with an airfoil like the N.A.C.A. 2412-34 from the family of reference 3. This type of airfoil has a better lift-load distribution and a thickness distribution that does not produce a minimum-pressure peak excessively far forward. The N.A.C.A. 2412-34 and N.A.C.A. 1412-34 airfoils are therefore to be tested in the new tunnel and will be separately reported when the results are available.

It should be urged, however, that snap judgments based on boundary-layer calculations along the lines suggested by reasoning similar to that presented in the preceding paragraphs be withheld pending further experimental investigations. Some of the test results (figs. 15 and 26, for example) show large drag increases associated with comparatively small forward movements of the transition point. The cause of this rather peculiar behavior of the drag was found, as the result of a supplementary investigation to be separately reported, to be associated with the very high skin-friction intensities usually present at the onset of turbulence in the boundary layer. The adverse effects of the high friction intensities are moderated, however, when the transition occurs in a region of pressure recovery as it does on the best sections in the optimum operating condition. In fact, the type of flow leading to a relatively high intensity skin friction is then actually desirable in order to avoid separation. It thus appears that it may always be desirable to effect some pressure recovery in the neighborhood of the transition point, not only because of the immediate saving in skin friction and lower losses associated with recovery but also because the turbulent layer is left to run over the remainder of the airfoil in a thicker, and hence lower, drag condition.

The same conclusion was reached in a different way,

which actually led to the design of the 0.5c-chord extension on the N.A.C.A. 27-215 airfoil. If chords longer than the optimum, that is higher Reynolds Numbers must be employed, the least adverse drag effects should be expected when the best possible section is chosen for the forward part of the airfoil and the remainder, which must be exposed to turbulent skin friction anyway, is added as a relatively thin extension lying in the wake of the forward part where the velocities and turbulent-friction intensities are a minimum. Although the test results in figure 24 cannot be said to substantiate these views, neither can they be said to disprove them. Owing to the larger chord and the resulting different relative position of the survey rake, the results for this airfoil should not be considered strictly comparable, and conclusions should be withheld pending further tests. It is apparent, nevertheless, that drag gains will be much less marked if any large forward movement of the transition point is allowed to result from increasing values of the Reynolds Number.

### CONCLUSION

For airplane wing design and for other airfoil and streamline body applications in the lower Reynolds Number range the new laminar-flow airfoils and the general design principles deduced from the present investigations may be expected to yield actual wing-drag coefficients markedly smaller than those heretofore possible.

Airfoil and flow investigations of the type considered must be made under tunnel-flow conditions approaching freedom from turbulence. Under these suitable conditions, truly laminar-boundary layers may be maintained to unusually high values of the Reynolds Number. Transition appears to be sensitive to very small disturbances of various kinds including surface roughness and air-stream turbulence and, in the absence of such disturbances, appears to be of a different character from that usually observed in wind-tunnel testing.

Langley Memorial Aeronautical Laboratory,  
National Advisory Committee for Aeronautics,  
Langley Field, Va., April 25, 1939.

## REFERENCES

1. Stüper, J.: Investigation of Boundary Layers on an Airplane Wing in Free Flight. T.M. No. 751, N.A.C.A., 1934.
2. Jones, Melvill: Flight Experiments on the Boundary Layer. Jour. Aero. Sci., vol. 5, no. 3, Jan. 1938, pp. 81-94.
3. Stack, John, and von Doenhoff, Albert E.: Tests of 16 Related Airfoils at High Speeds. T.R. No. 492, N.A.C.A., 1934.
4. Jacobs, Eastman N., and Clay, William C.: Characteristics of the N.A.C.A. 23012 Airfoil from Tests in the Full-Scale and Variable-Density Tunnels. T.R. No. 530, N.A.C.A., 1935.
5. von Doenhoff, Albert E.: A Preliminary Investigation of Boundary-Layer Transition along a Flat Plate with Adverse Pressure Gradient. T.N. No. 639, N.A.C.A., 1938.
6. Jacobs, Eastman N.: Laminar and Turbulent Boundary Layers as Affecting Practical Aerodynamics. S.A.E. Jour., vol. 41, no. 4, Oct. 1937, pp. 468-472.
7. Theodorsen, Theodore: Theory of Wing Sections of Arbitrary Shapes. T.R. No. 411, N.A.C.A., 1931.
8. Jacobs, Eastman N., Ward, Kenneth E., and Pinkerton, Robert M.: The Characteristics of 78 Related Airfoil Sections from Tests in the Variable-Density Wind Tunnel. T.R. No. 460, N.A.C.A., 1933.
9. Dryden, Hugh L.: Turbulence and the Boundary Layer. Jour. Aero. Sci., vol. 6, no. 3, Jan. 1939, pp. 85-100.
10. Allen, H. Julian: A Simplified Method for Calculation of Airfoil Pressure Distribution. T.M. No. 708, N.A.C.A., 1939.
11. Jacobs, Eastman N.: Methods Employed in America for the Experimental Investigation of Aerodynamic Phenomena at High Speeds. Misc. Paper No. 42, N.A.C.A., 1936.

12. von Doenhoff, Albert E., and Jacobs, Eastman N.: Transition as It Occurs Associated with and Following Laminar Separation. (Paper Presented before Fifth International Congress for Applied Mechanics, Cambridge, Mass., Sept. 12-16, 1938.)
13. von Doenhoff, Albert E.: A Method of Rapidly Estimating the Position of the Laminar Separation Point. T.N. No. 671, N.A.C.A., 1938.
14. Silverstein, Abe, and Becker, John V.: Determination of Boundary-Layer Transition on Three Symmetrical Airfoils in the N.A.C.A. Full-Scale Wind Tunnel. T.R. No. 637, N.A.C.A., 1939.
15. Jacobs, Eastman N., and Rhode, R. V.: Airfoil Section Characteristics as Applied to the Prediction of Air Forces and Their Distribution on Wings. T.R. No. 631, N.A.C.A., 1938.

TABLE I  
Mean Line Ordinates and Slopes

Station % c	Const. load type		Load const. to 3c		N.A.C.A. 27-215 with .5c extension	
	N.A.C.A. 16-series, etc.	Slope	N.A.C.A. 27-series, etc.	Slope	N.A.C.A. 27-012 with .5c ext.	Slope
0	0	—	0	—	0	—
.3	.032	.09238	.037	.10615	.056	.15813
.6	.059	.08133	.066	.09383	.093	.13985
1.25	.107	.06954	.123	.08073	.183	.11984
2.5	.186	.05831	.215	.06823	.320	.10088
5.0	.316	.04686	.367	.05546	.545	.08131
7.5	.424	.03999	.496	.04775	.734	.06932
10	.517	.03497	.606	.04216	.894	.06038
15	.673	.02761	.798	.03376	1.161	.04681
20	.796	.02206	.948	.02748	1.367	.03603
25	.895	.01749	1.074	.02220	1.523	.02653
30	.972	.01349	1.173	.01753	1.633	.01755
35	1.030	.00985	1.252	.01326	1.699	.00852
40	1.071	.00645	1.306	.00918	1.717	-.00113
45	1.095	.00319	1.343	.00382	1.685	-.01230
50	1.103	0	1.357	.00124	1.588	-.02723
55	1.095	-.00319	1.353	-.00286	1.385	-.05634
60	1.071	-.00645	1.329	-.00721	1.069	-.06702
65	1.030	-.00985	1.284	-.01201	.742	-.06077
70	.972	-.01349	1.208	-.01756	.507	-.03615
75	.895	-.01749	1.100	-.02460	.354	-.02585
80	.796	-.02206	.954	-.03681	.242	-.01951
85	.673	-.02761	.752	-.04784	.155	-.01501
90	.517	-.03497	.486	-.05119	.089	-.01159
92	.444	-.03887	.380	-.05119	.067	-.01044
94	.361	-.04379	.273	-.05047	.048	-.00938
95	.316	-.04686	.220	-.04981	.038	-.00888
96	.267	-.05058	.173	-.04889	.030	-.00840
98	.156	-.06194	.082	-.04616	.014	-.00750
100	0	—	0	-.04076	0	-.00666

$c_x = .2$  at  $\alpha = 0^\circ$

$c_x = .2$  at  $\alpha = .3^\circ$

$c_x = .13$  at  $\alpha = .10^\circ$

TABLE II  
Basic Thickness Ordinates

Station % c	Ordinates - percent chord					
	N.A.C.A. 07-012	N.A.C.A. 16-012	N.A.C.A. 27-012	N.A.C.A. 18-012	N.A.C.A. 19-012	N.A.C.A. 27-012 with .5c ext.
0	0	0	0	0	0	0
.3		.642	.640	.587	.544	
.6		.902	.885	.826	.765	
1.25	1.640	1.292	1.271	1.182	1.096	1.550
2.5	2.227	1.806	1.778	1.654	1.536	2.161
5.0	2.920	2.510	2.464	2.303	2.140	2.967
7.5	3.440	3.032	2.965	2.786	2.593	3.559
10	3.867	3.458	3.373	3.182	2.964	4.034
15	4.547	4.134	4.032	3.819	3.566	4.770
20	5.053	4.664	4.544	4.325	4.048	5.302
25	5.427	5.085	4.963	4.740	4.452	5.683
30	5.693	5.417	5.299	5.085	4.794	5.917
35		5.673	5.567	5.368	5.085	6.000
40	5.947	5.854	5.769	5.600	5.331	5.940
45		5.964	5.908	5.773	5.536	5.650
50	5.993	6.000	5.990	5.899	5.703	5.078
55		5.961	6.000	5.975	5.833	4.121
60	5.827	5.834	5.936	6.000	5.925	3.112
65		5.609	5.766	5.971	5.981	2.317
70	5.334	5.270	5.499	5.862	6.000	1.660
75		4.804	5.097	5.638	5.975	1.183
80	4.453	4.198	4.509	5.246	5.858	.804
85		3.441	3.632	4.615	5.551	.509
90	2.547	2.518	2.486	3.648	4.843	.286
92		2.098	1.972	3.139	4.366	
94		1.650	1.455	2.543	3.721	
95	1.333	1.414		2.210	3.317	.115
96		1.172	.935	1.852	2.850	
98		.662	.426	1.049	1.684	
100	0	0	0	0	0	0
L.E. Rad.	1.33	.71	.70	.50	.37	.47

TABLE III  
Basic Pressure Distribution

Station %c	Values of pressure coefficient, "s"					
	N.A.C.A. 07-004	N.A.C.A. 07-006	N.A.C.A. 07-009	N.A.C.A. 07-012	N.A.C.A. 07-015	N.A.C.A. 07-018
0	0	0	0	0	0	0
1.25	1.085	1.122	1.164	1.158	1.058	0.807
2.5	1.088	1.129	1.183	1.230	1.242	1.231
5.0	1.089	1.134	1.190	1.238	1.275	1.300
7.5	1.089	1.134	1.192	1.243	1.284	1.315
10	1.090	1.135	1.200	1.255	1.304	1.345
15	1.091	1.137	1.207	1.274	1.337	1.396
20	1.083	1.140	1.211	1.283	1.353	1.423
30	1.082	1.138	1.206	1.277	1.351	1.429
40	1.089	1.133	1.199	1.267	1.340	1.415
50	1.087	1.130	1.196	1.263	1.334	1.410
60	1.087	1.130	1.196	1.263	1.334	1.410
70	1.089	1.134	1.200	1.267	1.337	1.412
80	1.079	1.119	1.179	1.236	1.295	1.354
90	1.031	1.045	1.055	1.055	1.035	.995
95	1.015	1.020	1.015	.990	.928	.804
100	0	0	0	0	0	0

TABLE V  
Basic Pressure Distribution

Station %c	Values of pressure coefficient, "s"					
	N.A.C.A. 27-004	N.A.C.A. 27-006	N.A.C.A. 27-009	N.A.C.A. 27-012	N.A.C.A. 27-015	N.A.C.A. 27-018
0	0	0	0	0	0	0
1.25	1.042	1.053	1.052	1.024	0.961	0.890
2.5	1.056	1.084	1.117	1.134	1.117	1.059
5.0	1.061	1.092	1.138	1.176	1.207	1.230
7.5	1.065	1.098	1.147	1.196	1.241	1.286
10	1.068	1.102	1.154	1.205	1.257	1.309
15	1.071	1.107	1.161	1.215	1.271	1.327
20	1.075	1.112	1.168	1.225	1.283	1.345
30	1.081	1.121	1.182	1.245	1.310	1.380
40	1.087	1.130	1.197	1.264	1.337	1.416
50	1.094	1.140	1.210	1.284	1.365	1.451
60	1.099	1.149	1.222	1.302	1.390	1.486
70	1.102	1.155	1.233	1.317	1.409	1.512
80	1.092	1.138	1.208	1.281	1.360	1.443
90	1.022	1.029	1.029	1.015	.984	.930
95	.936	.905	.858	.806	.751	.683
100	0	0	0	0	0	0

NATIONAL ADVISORY  
COMMITTEE FOR AERONAUTICS  
CONFIDENTIAL

TABLE IV  
Basic Pressure Distribution

Station %c	Values of pressure coefficient, "s"					
	N.A.C.A. 16-004	N.A.C.A. 16-006	N.A.C.A. 16-009	N.A.C.A. 16-012	N.A.C.A. 16-015	N.A.C.A. 16-018
0	0	0	0	0	0	0
1.25	1.041	1.050	1.047	1.015	.953	.834
2.5	1.059	1.085	1.111	1.125	1.117	1.075
5.0	1.065	1.097	1.141	1.181	1.210	1.227
7.5	1.068	1.101	1.150	1.198	1.238	1.273
10	1.070	1.105	1.159	1.209	1.256	1.298
15	1.075	1.111	1.169	1.224	1.279	1.330
20	1.078	1.117	1.176	1.235	1.294	1.351
30	1.081	1.124	1.188	1.254	1.321	1.392
40	1.086	1.130	1.197	1.268	1.345	1.428
50	1.091	1.137	1.207	1.283	1.365	1.451
60	1.095	1.143	1.218	1.295	1.373	1.451
70	1.094	1.139	1.206	1.278	1.342	1.401
80	1.069	1.104	1.156	1.205	1.251	1.299
90	1.018	1.025	1.032	1.035	1.031	1.020
95	.982	.969	.943	.906	.852	.779
100	0	0	0	0	0	0

TABLE VI  
Basic Pressure Distribution

Station %c	Values of pressure coefficient, "s"					
	N.A.C.A. 18-004	N.A.C.A. 18-006	N.A.C.A. 18-009	N.A.C.A. 18-012	N.A.C.A. 18-015	N.A.C.A. 18-018
0	0	0	0	0	0	0
1.25	1.007	1.009	1.000	0.968	0.904	0.805
2.5	1.026	1.040	1.059	1.074	1.079	1.054
5.0	1.044	1.066	1.099	1.132	1.165	1.194
7.5	1.054	1.081	1.122	1.162	1.203	1.243
10	1.060	1.091	1.135	1.180	1.225	1.269
15	1.064	1.097	1.145	1.194	1.242	1.291
20	1.066	1.100	1.150	1.202	1.255	1.310
30	1.068	1.102	1.155	1.211	1.273	1.339
40	1.071	1.108	1.163	1.224	1.293	1.366
50	1.078	1.118	1.177	1.245	1.319	1.405
60	1.089	1.134	1.200	1.275	1.356	1.452
70	1.103	1.154	1.231	1.311	1.402	1.509
80	1.110	1.167	1.255	1.346	1.446	1.559
90	1.098	1.141	1.195	1.232	1.240	1.225
95	1.016	1.015	1.000	.975	.937	.870
100	0	0	0	0	0	0

N.A.C.A.

Tables 3, 4, 5, 6

TABLE VII

## Basic Pressure Distribution

Station percent c	Values of pressure coefficient "S"					
	N.A.C.A. 19-004	N.A.C.A. 19-006	N.A.C.A. 19-009	N.A.C.A. 19-012	N.A.C.A. 19-015	N.A.C.A. 19-018
0	0	0	0	0	0	0
1.25	1.009	1.010	1.000	0.989	0.972	0.955
2.5	1.027	1.039	1.056	1.075	1.092	1.106
5.0	1.044	1.065	1.097	1.129	1.162	1.197
7.5	1.050	1.075	1.113	1.151	1.190	1.230
10	1.053	1.080	1.121	1.161	1.202	1.246
15	1.056	1.085	1.126	1.170	1.214	1.260
20	1.057	1.087	1.130	1.175	1.222	1.272
30	1.060	1.091	1.138	1.188	1.242	1.300
40	1.064	1.097	1.146	1.201	1.261	1.328
50	1.070	1.105	1.159	1.218	1.285	1.360
60	1.079	1.118	1.177	1.240	1.311	1.395
70	1.095	1.141	1.210	1.285	1.355	1.455
80	1.129	1.195	1.297	1.404	1.518	1.651
90	1.172	1.259	1.392	1.515	1.625	1.709
95	1.091	1.135	1.195	1.239	1.263	1.264
100	0	0	0	0	0	0

Figure 1.-Airfoil set-up in the model of the 2-dimensional-flow tunnel.

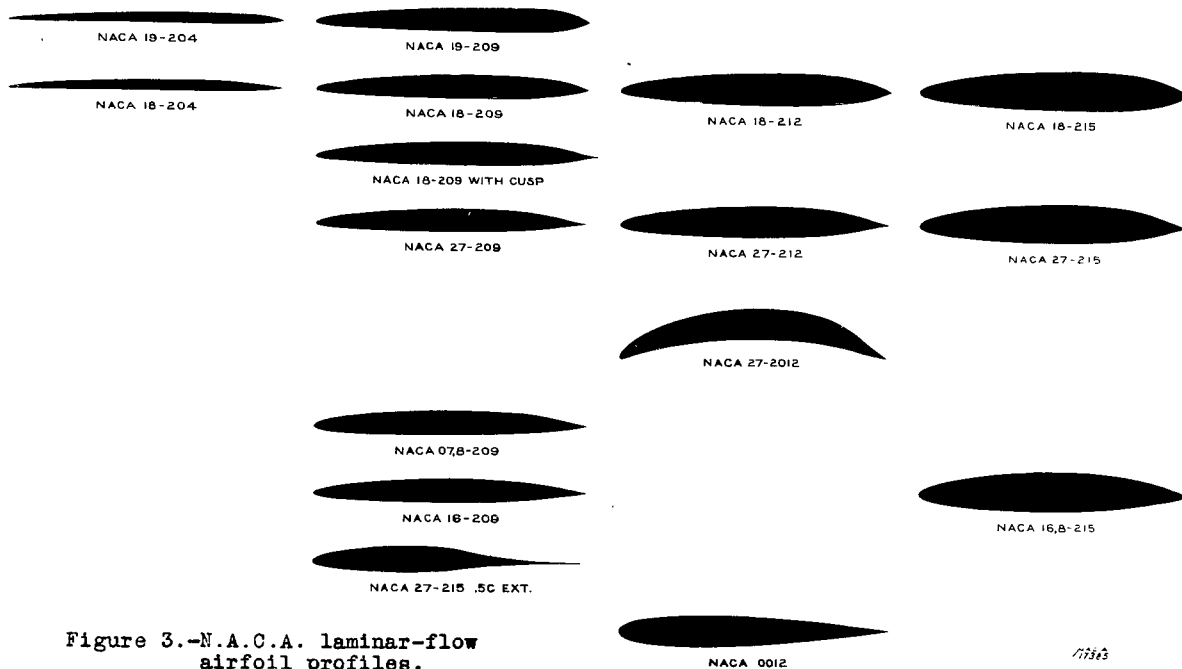


Figure 3.-N.A.C.A. laminar-flow airfoil profiles.

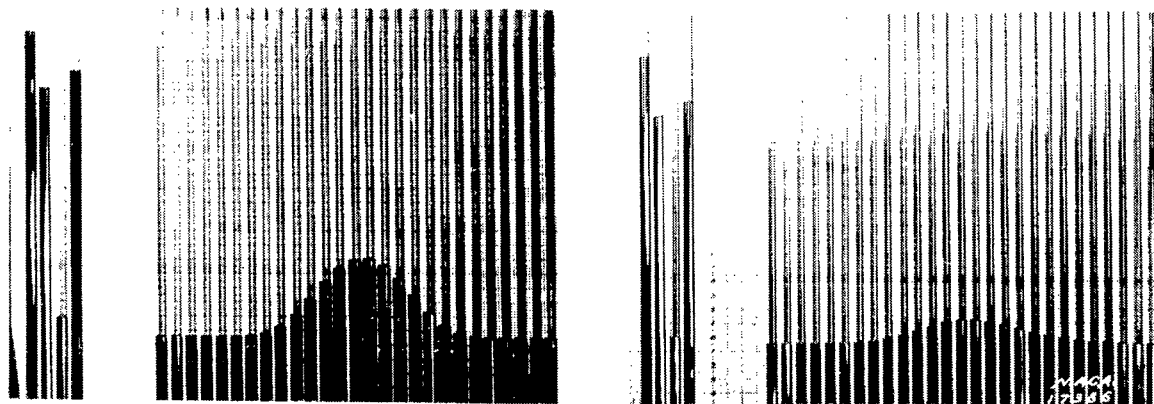


Figure 4.-Wake measurements by integrating manometer.

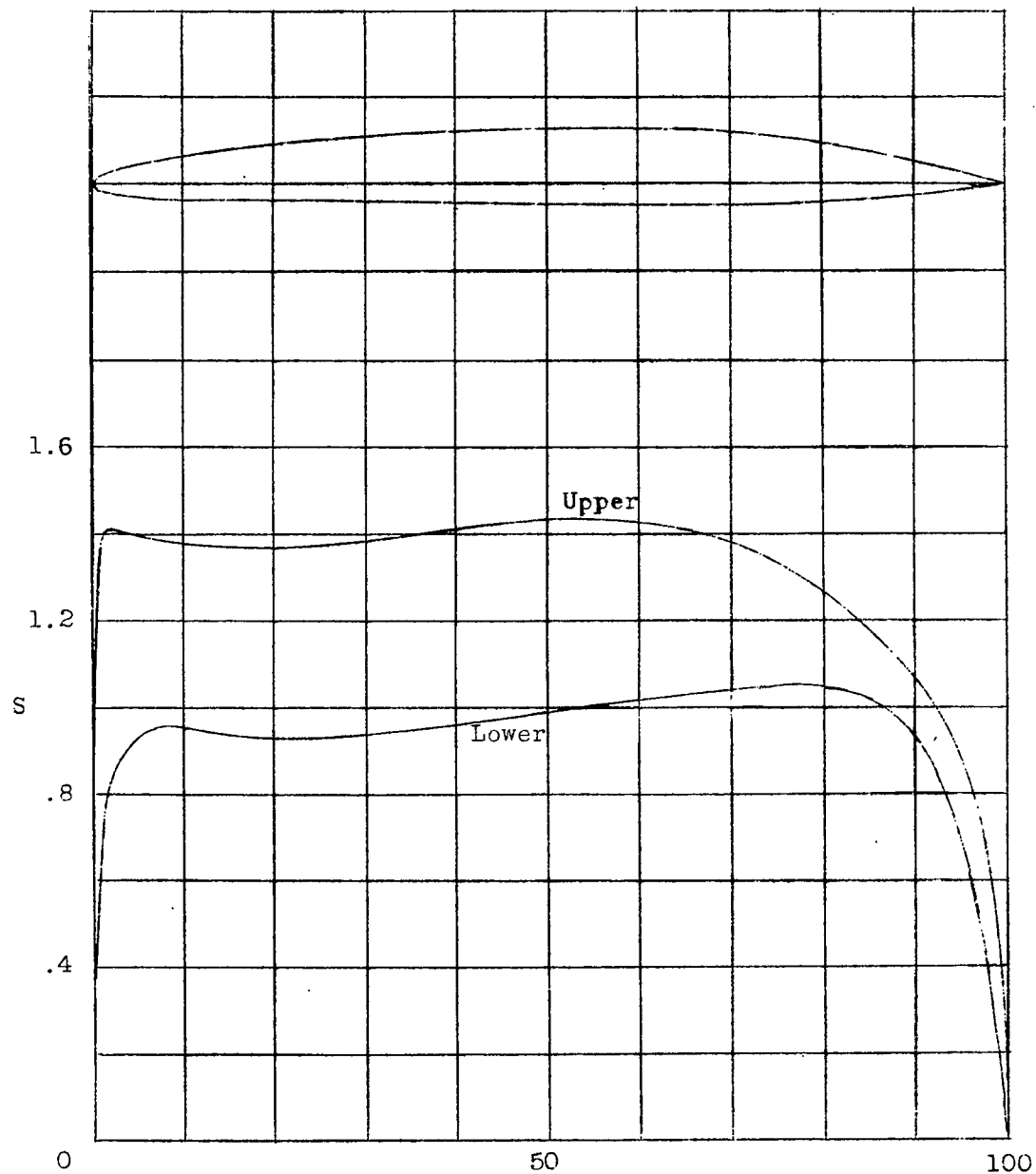


Figure 2.- Preliminary form of laminar-flow airfoil,  
(NACA 25 B 09-46).

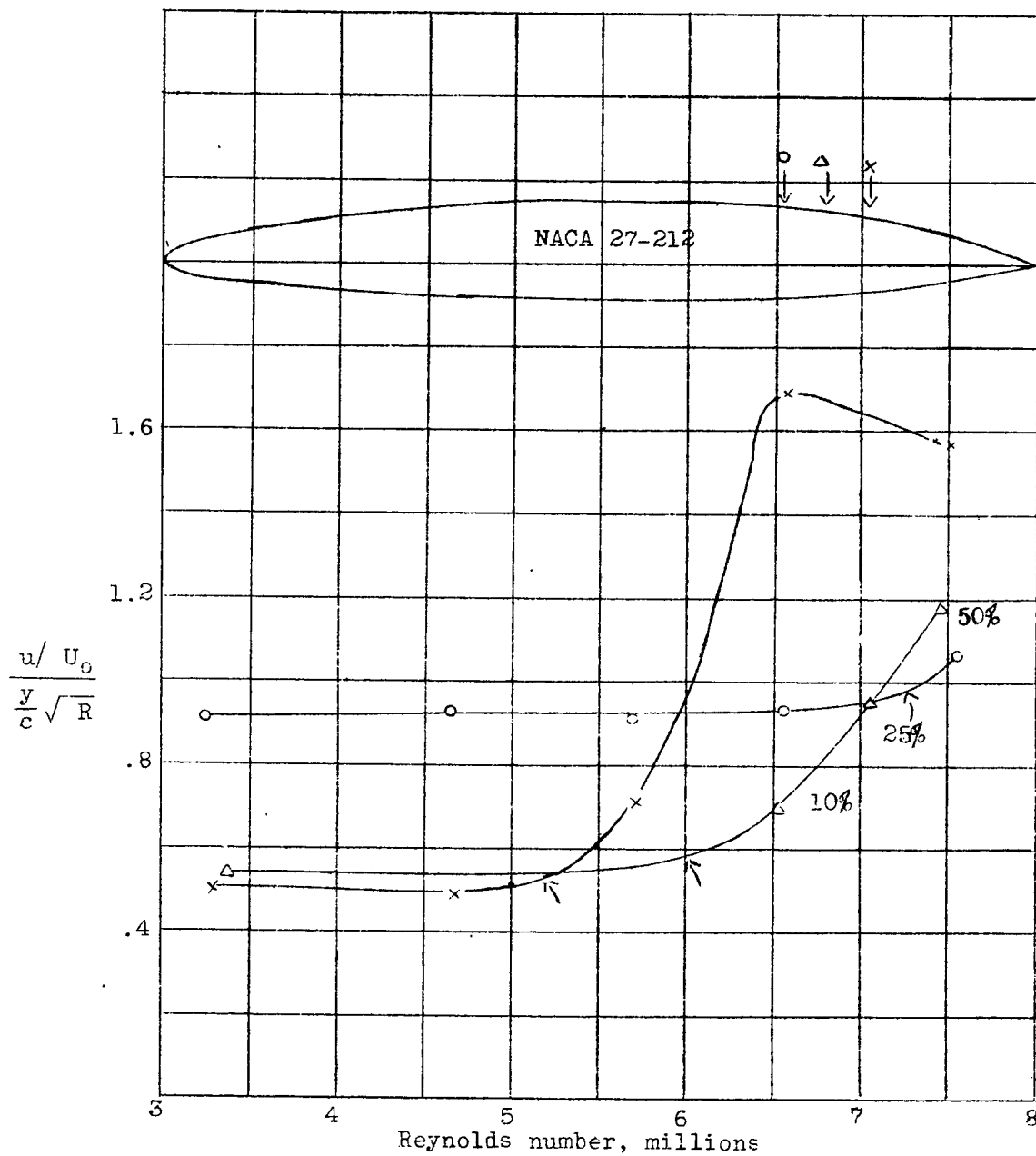
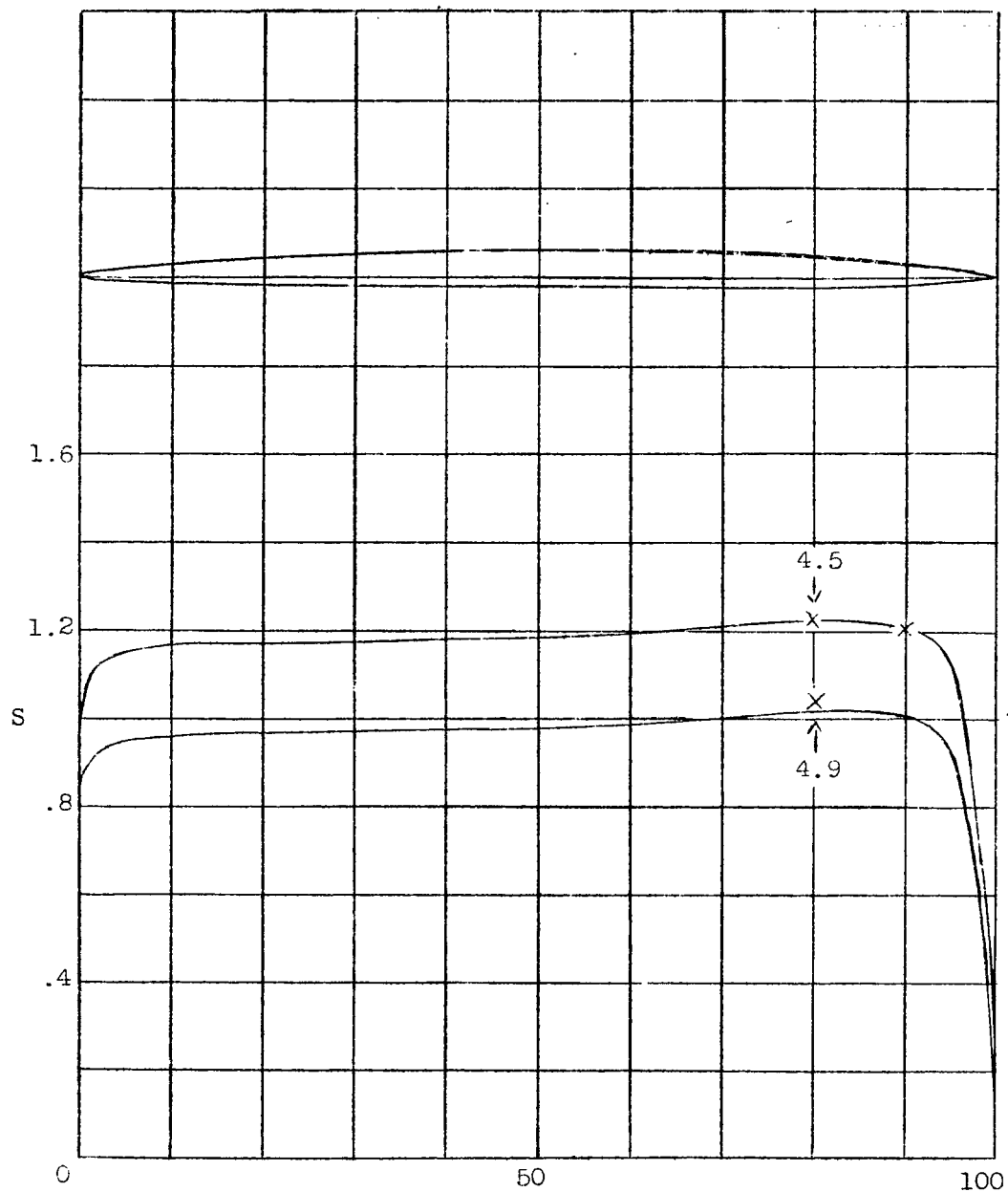
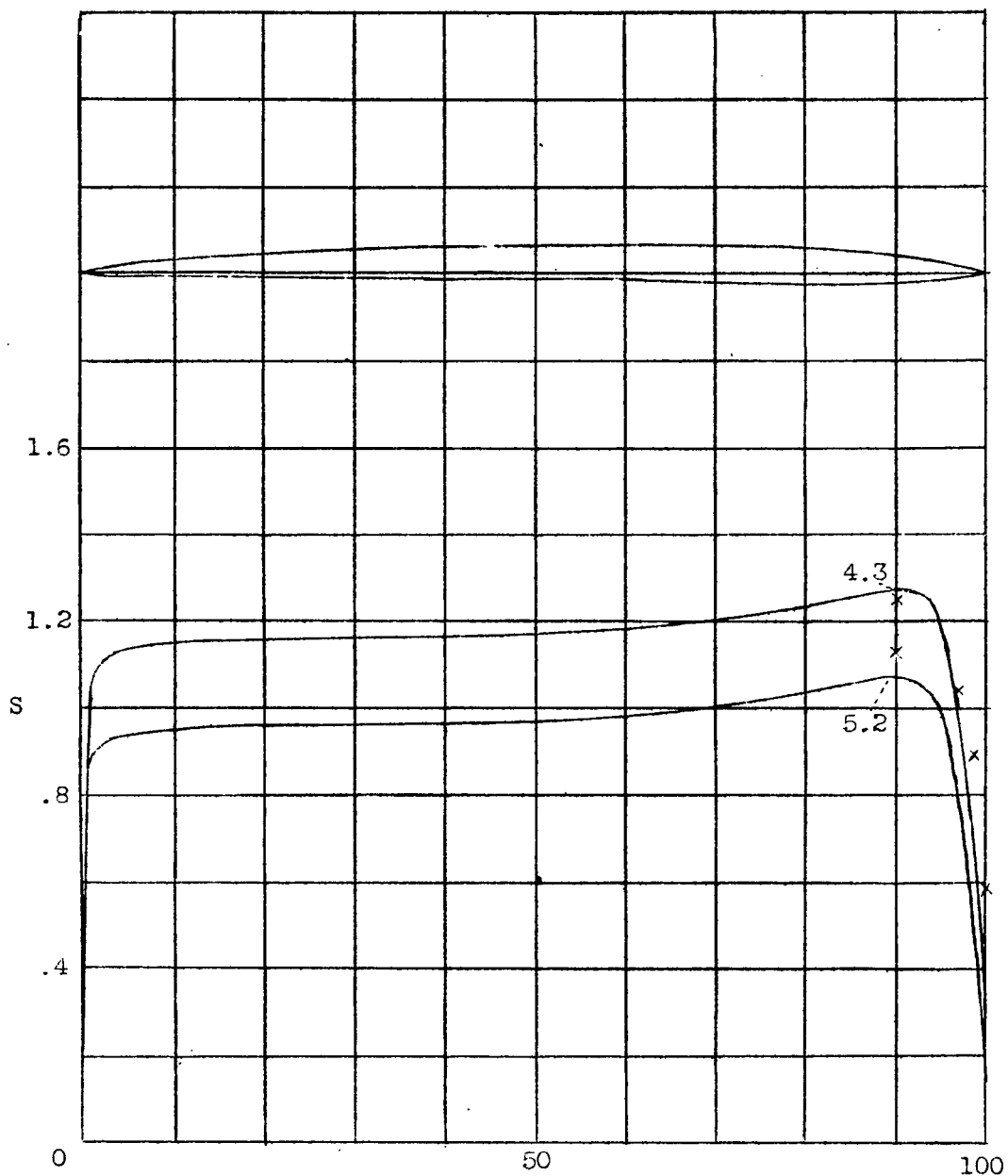


Figure 5.- Method of transition measurement. Variation of the "transition function" and correlation with hot-wire studies.



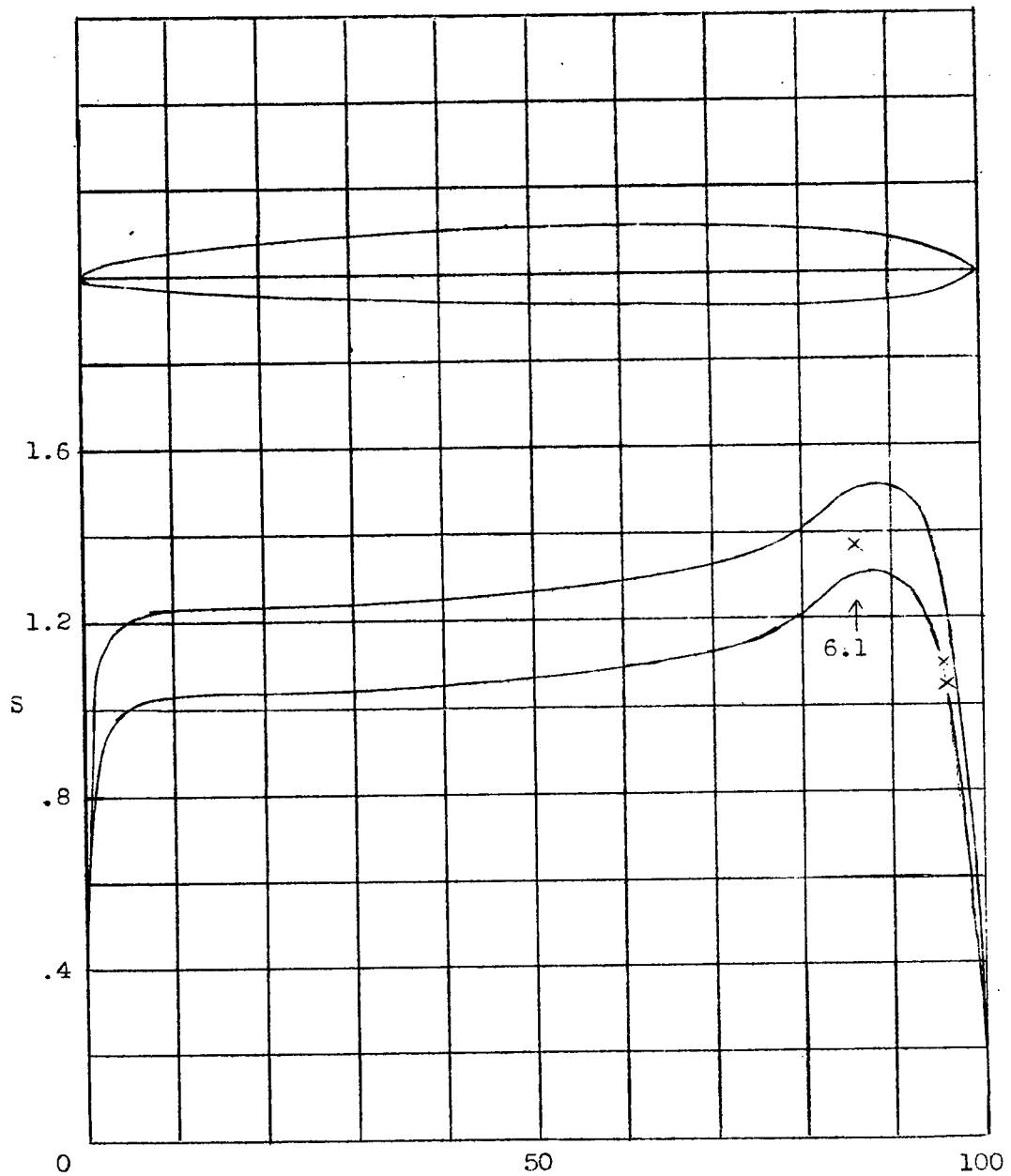
	$\alpha$	$c_l$	$M_c$	$c_{d_{min}}$
Theory	$0^\circ$	0.2	0.84	-
Experiment	$0^\circ$	-	.83	0.0022 at $R=4.2 \times 10^6$

Figure 6.- NACA 18-204 airfoil.



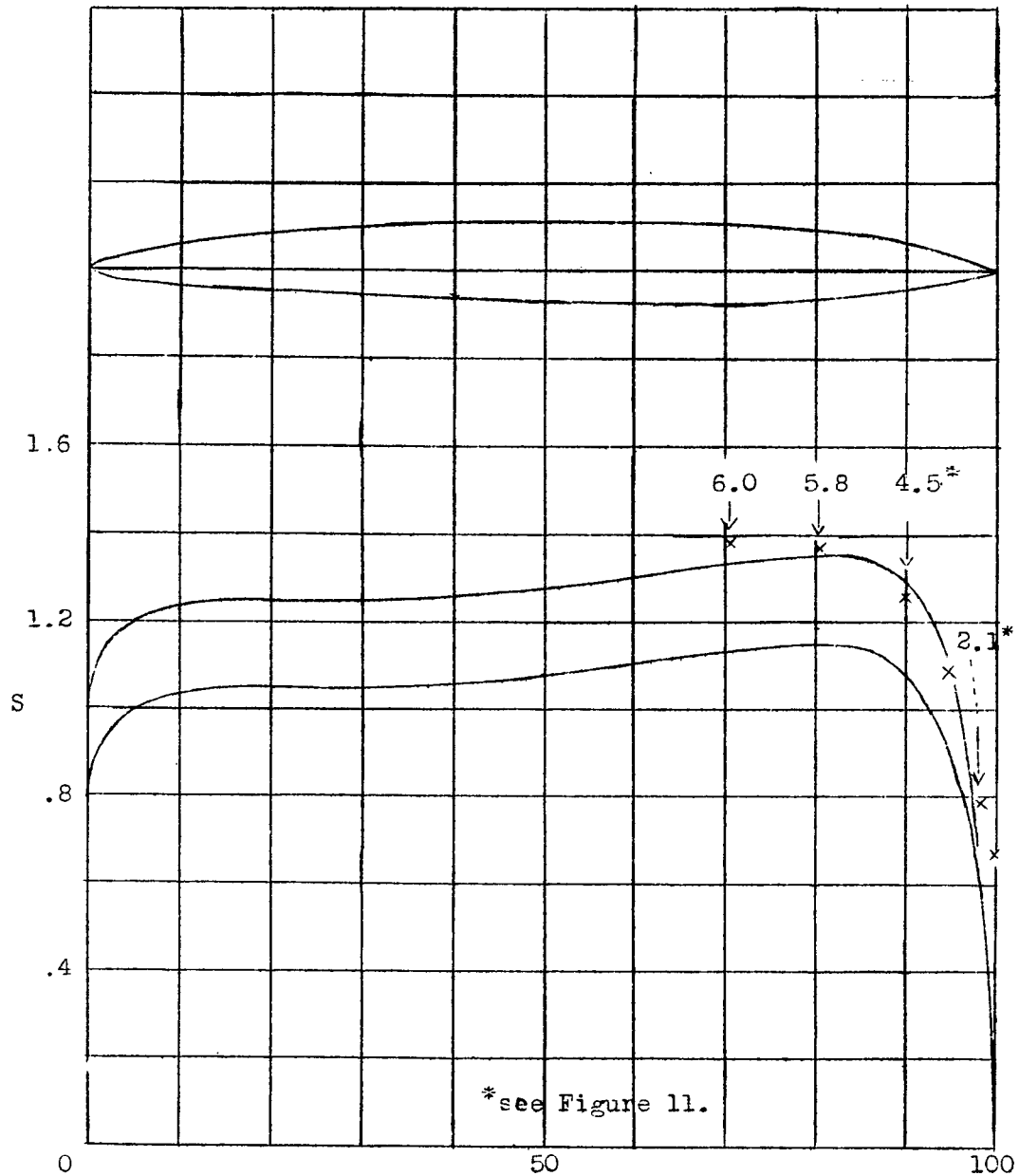
	$\alpha$	$C_l$	$M_c$	$C_{d_{min}}$
Theory	$0^\circ$	0.2	0.81	
Experiment	$1/2^\circ$	-	.82	0.0029 at $R=4.6 \times 10^6$

Figure 7.- NACA 19-204 airfoil.



	$\alpha$	$c_l$	$M_c$	$c_{d_{min}}$
Theory	$0^\circ$	0.2	0.71	-
Experiment	$1/2^\circ$	-	-	0.0039 at $R=4.6 \times 10^6$

Figure 8.- NACA 19-209 airfoil.



	$\alpha$	$c_l$	$M_c$	$c_{d_{min}}$
Theory	$0^\circ$	0.2	0.77	-
Experiment	$1/4^\circ$	-	.76	0.0026 at $R=5.3 \times 10^6$

Figure 9.-- NACA 18-209 airfoil.

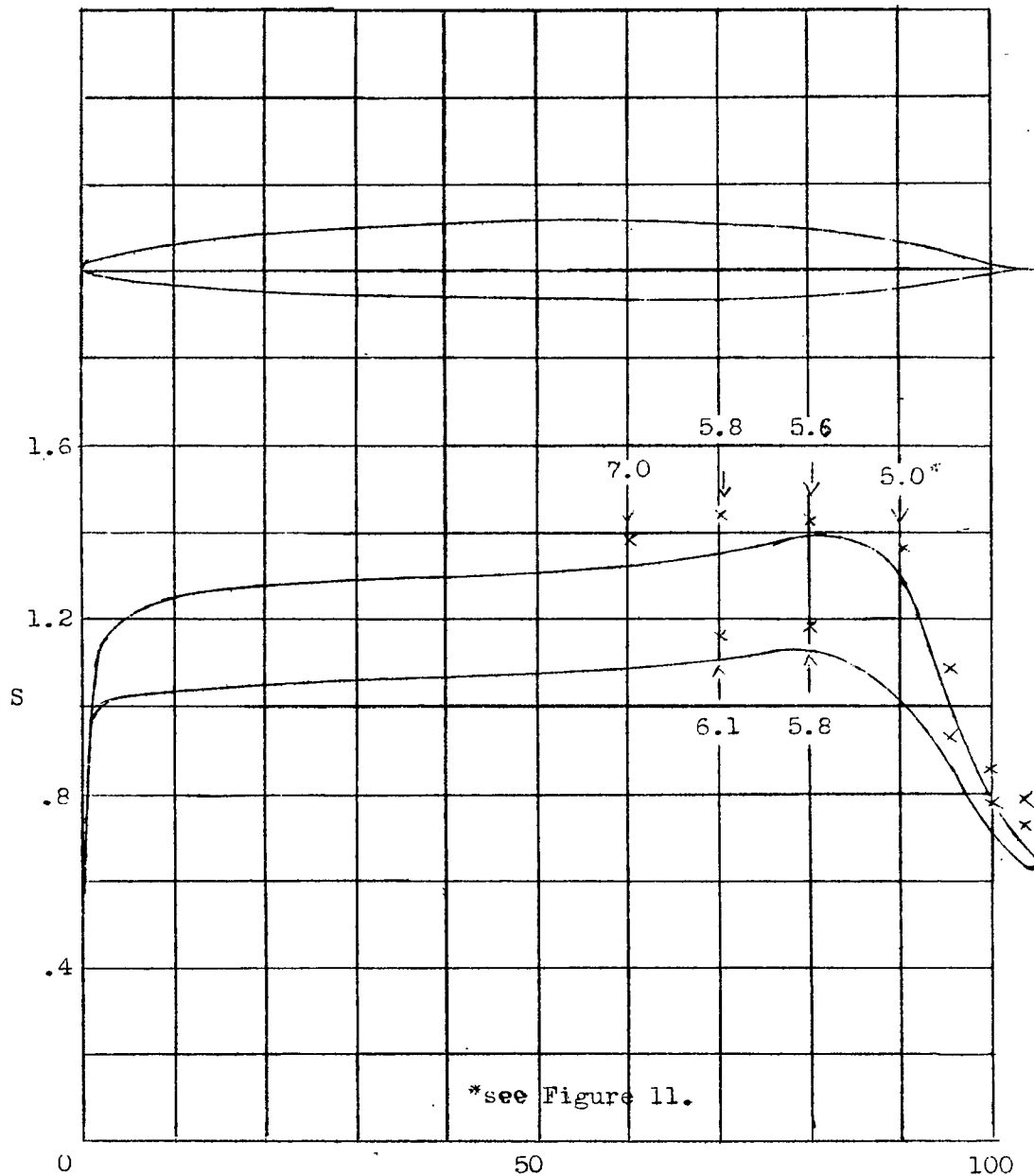
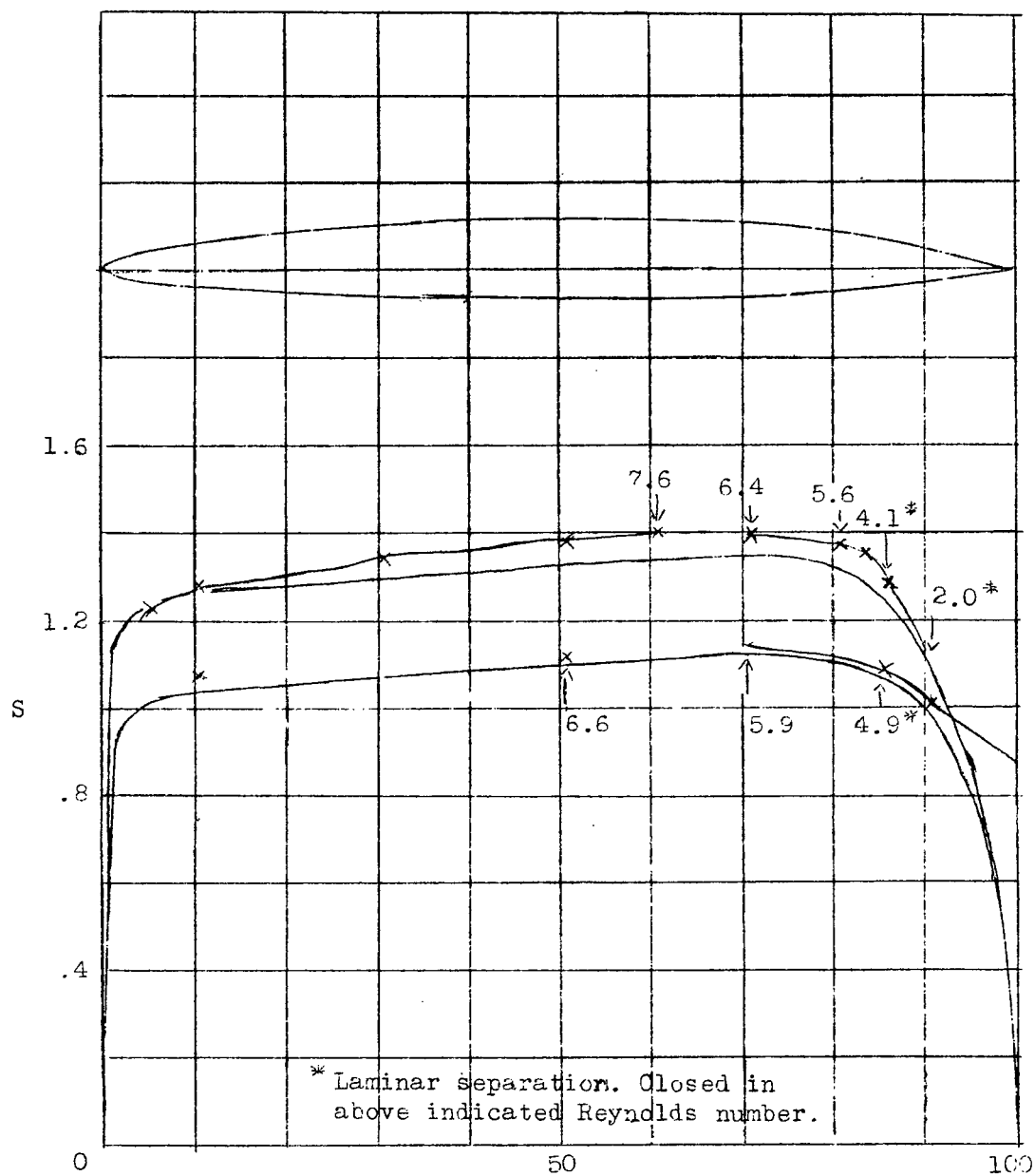


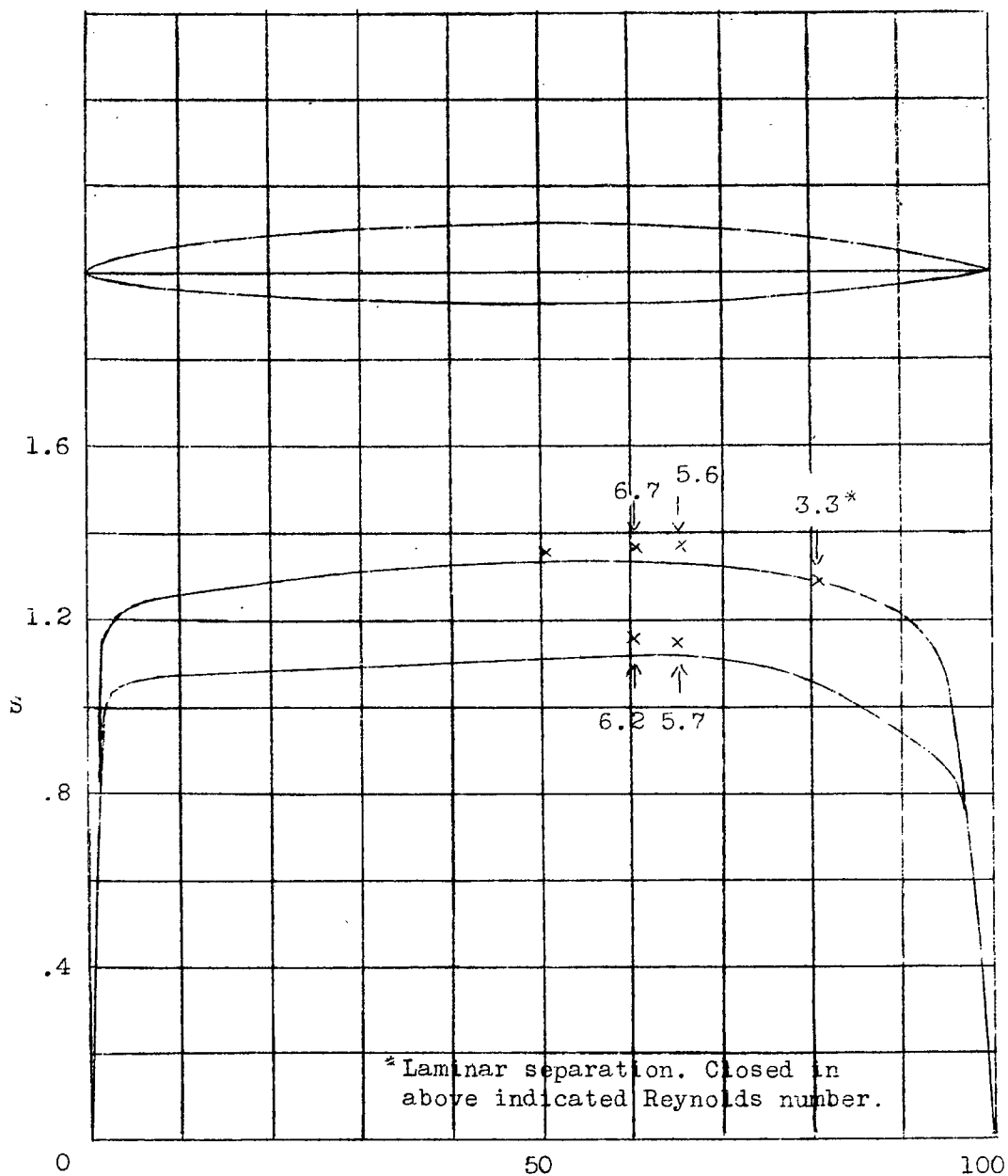
Figure 10.- NACA 18-209 airfoil with 3in cusp extension.



	$\alpha$	$c_l$	$M_c$	$c_{d_{min}}$
Theory	$0^\circ$	0.2	0.77	-
Experiment	$1/2^\circ$	.22	.75	0.0027 at $R=4.6 \times 10^6$

Arrows indicate location of transition corresponding to the Reynolds number indicated in millions.

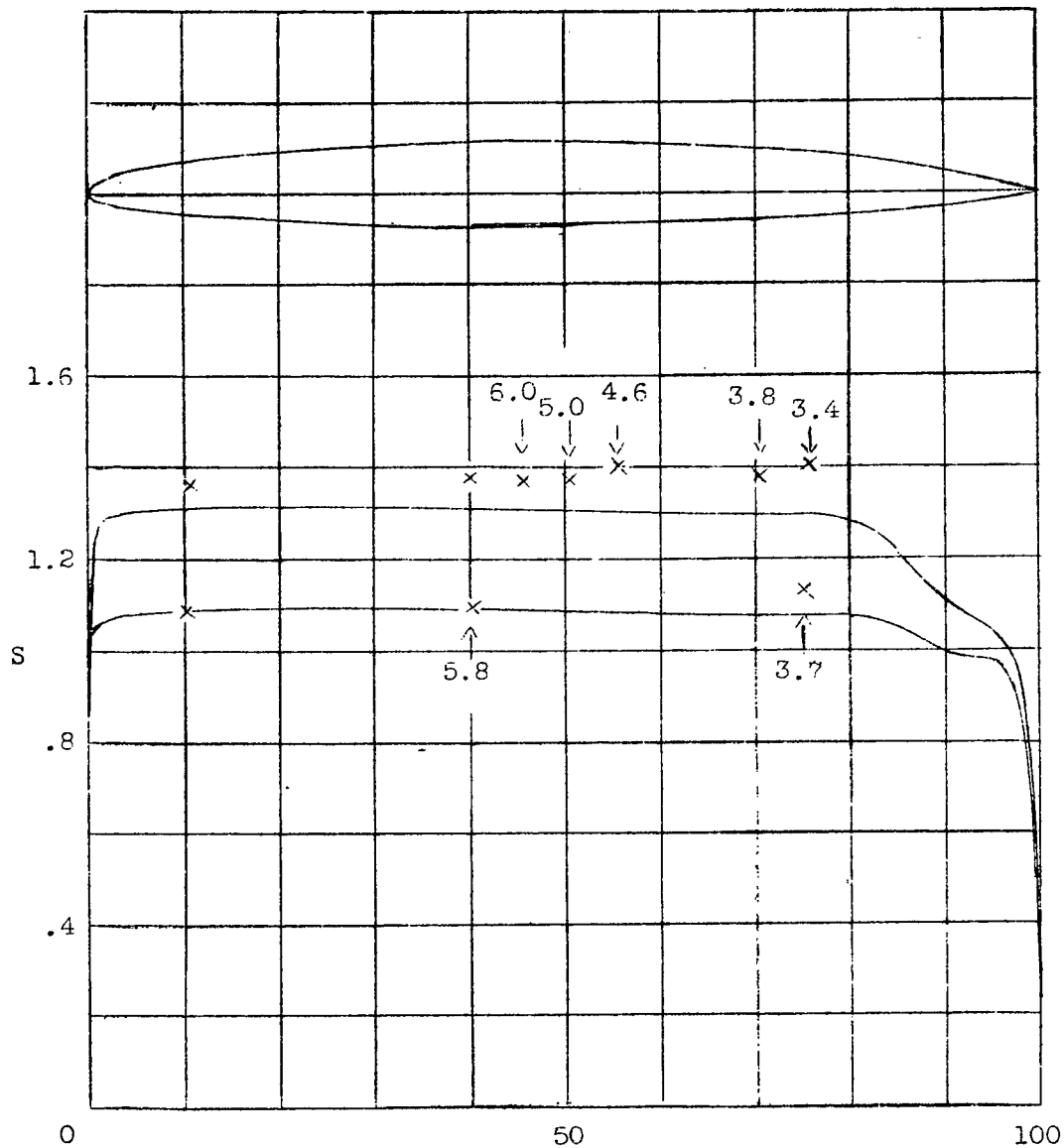
Figure 11.- NACA 27-209 airfoil.



	$\alpha$	$C_l$	$M_c$	$C_{d_{min}}$
Theory	$0^\circ$	0.2	0.78	-
Experiment	$0^\circ$	-	.76	0.0031 at $R=3.8 \times 10^6$

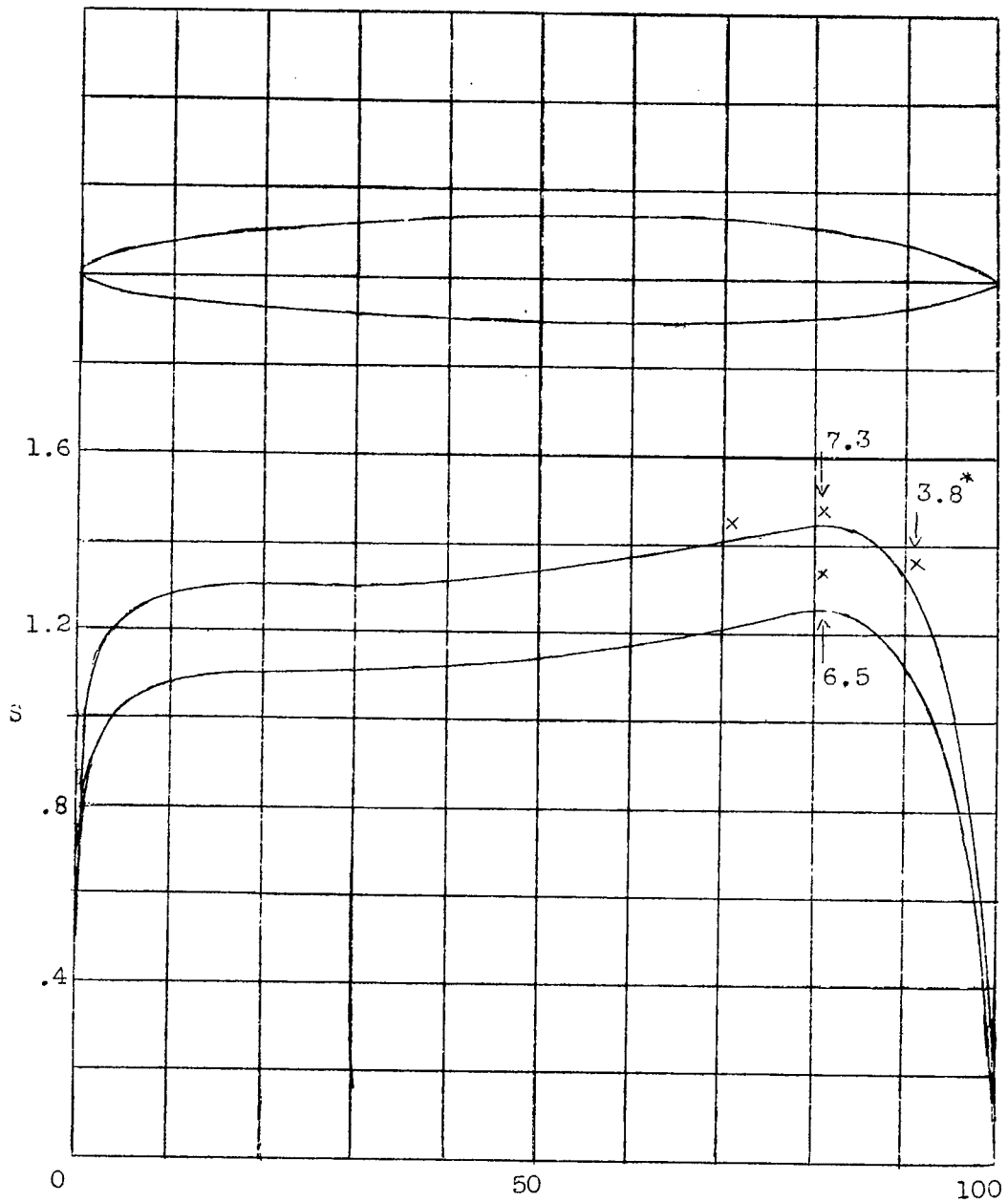
Arrows indicate location of transition corresponding to the Reynolds number in millions.

Figure 12.- NACA 16-209 airfoil.



	$\alpha$	$c_l$	$M_c$	$c_{d_{min}}$
Theory	$0^\circ$	0.2	0.79	-
Experimental	$1/2^\circ$	-	.75	$0.0034 \text{ at } R=3.3 \times 10^6$

Figure 13.- NACA 07,8-209 airfoil.



	$\alpha$	$C_l$	$M_c$	$C_{d_{min}}$
Theory	$0^\circ$	0.2	0.73	-
Experiment	$0^\circ$	-	.72	0.0033 at $R=5.3 \times 10^6$

Figure 14.- NACA 18-212 airfoil.

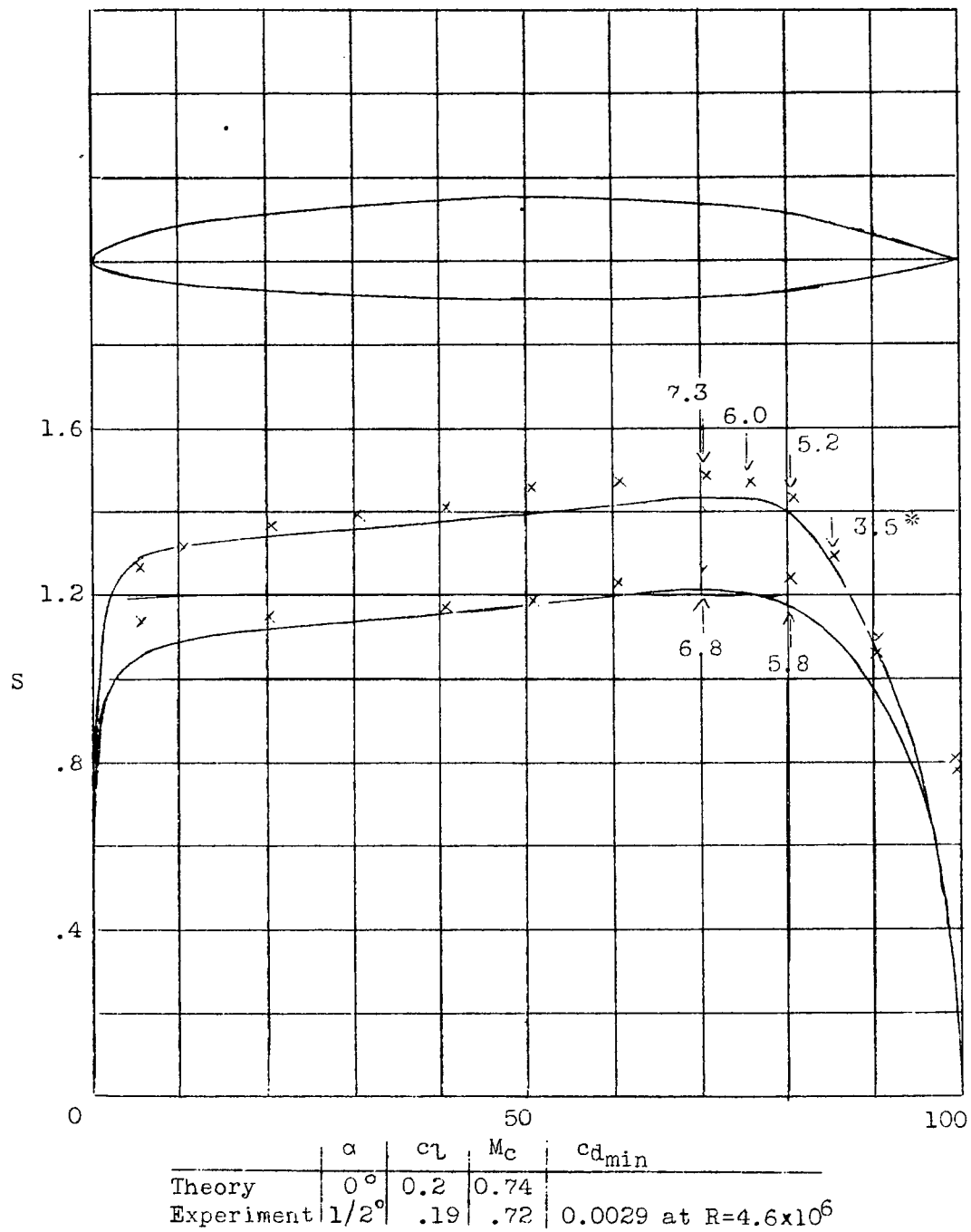


Figure 15.- NACA 27-212 airfoil.

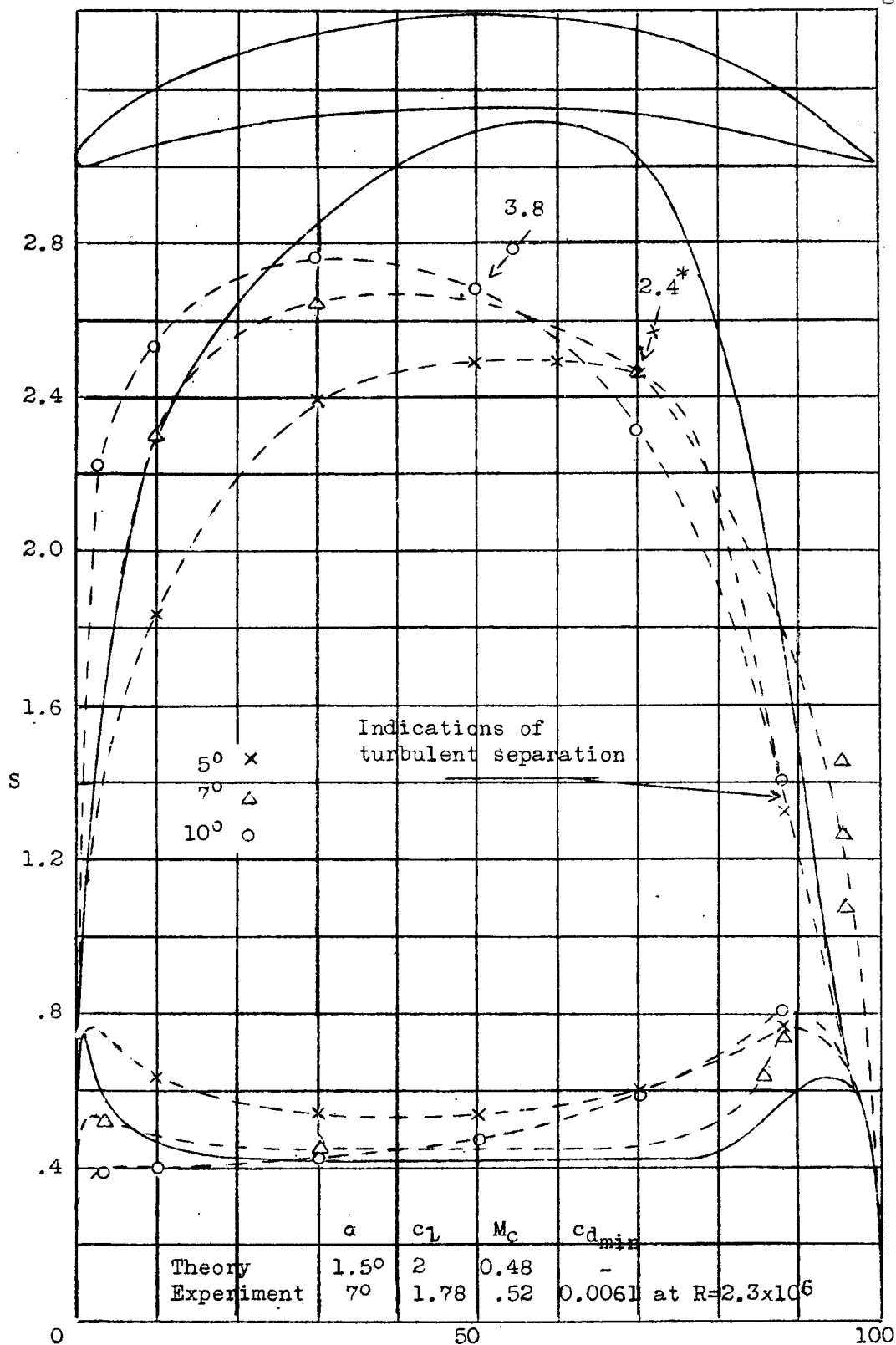
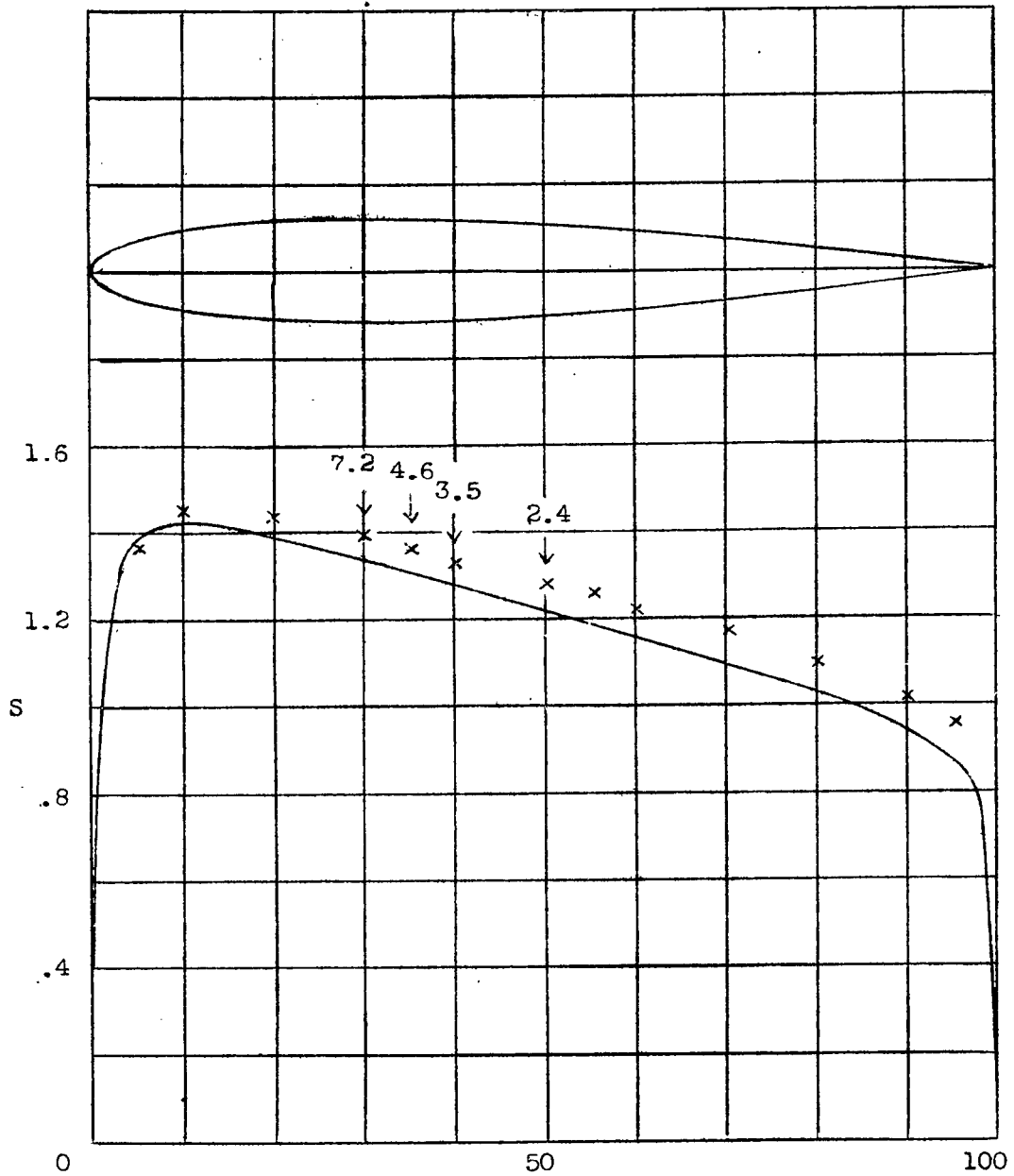
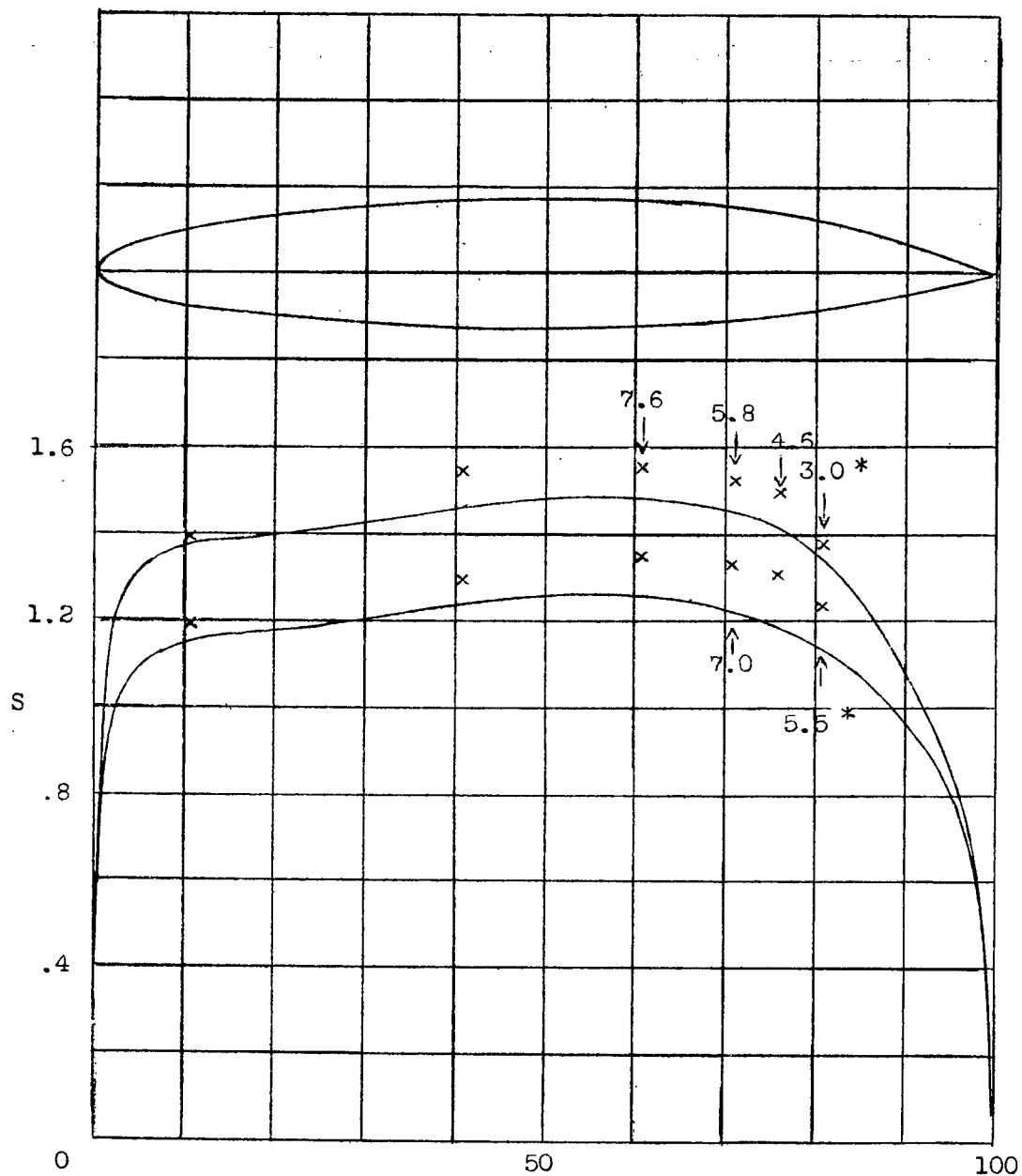


Figure 16.- NACA 27-2012 airfoil.



	$\alpha$	$C_L$	$M_c$	$C_{d_{min}}$
Theory	$0^\circ$	0	0.74	-
Experiment	$0^\circ$	0	.73	0.0071 at $R=4.6 \times 10^6$

Figure 17.- NACA 0012 airfoil.



	$\alpha$	$c_l$	$M_c$	$C_{d_{min}}$
Theory	$0^\circ$	0.2	0.72	-
Experiment	$1/2^\circ$	.18	.70	$0.0041$ at $R=4.6 \times 10^6$

Figure 18.- NACA 16,8-215 airfoil.

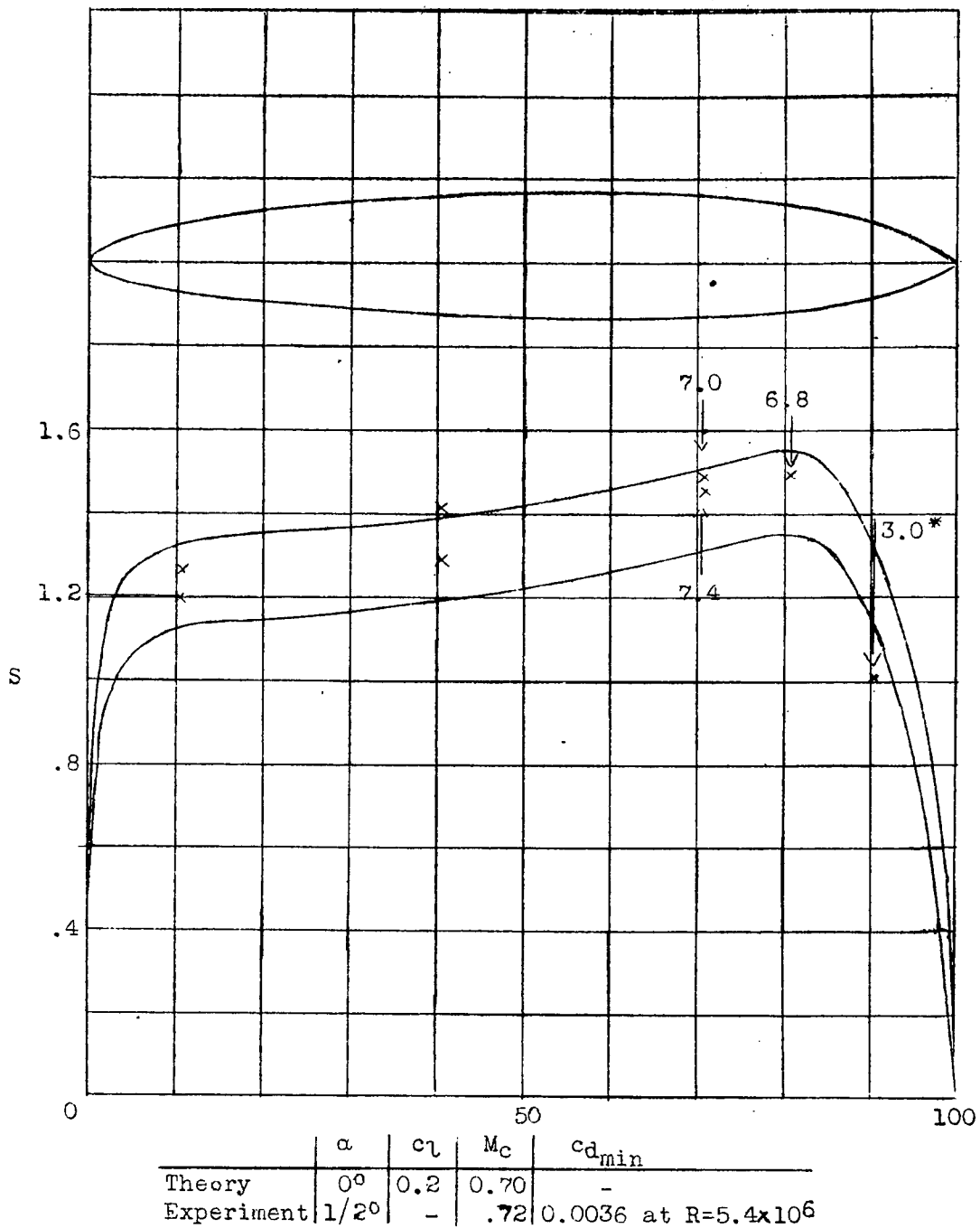


Figure 19.- NACA 18-215 airfoil.

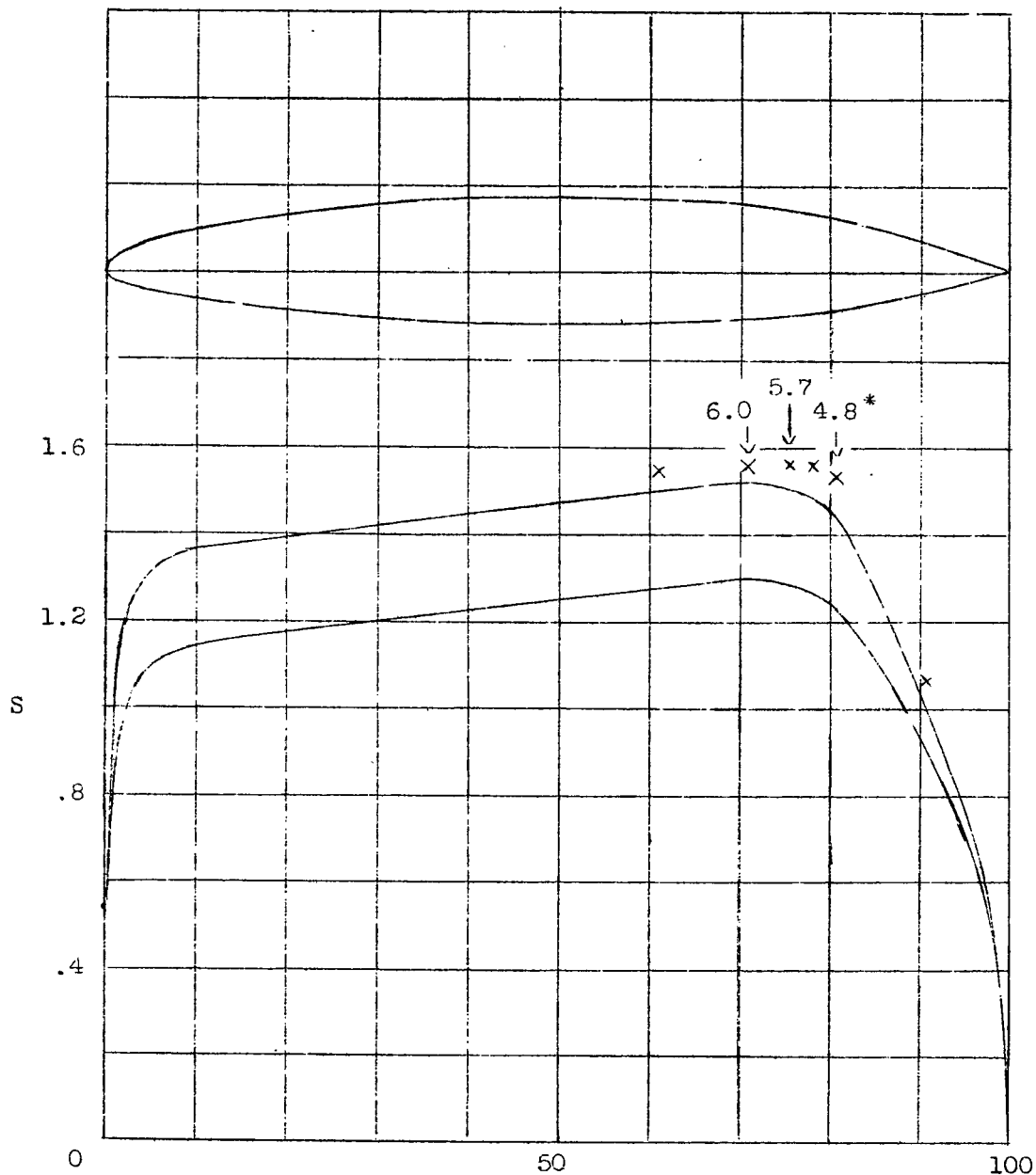
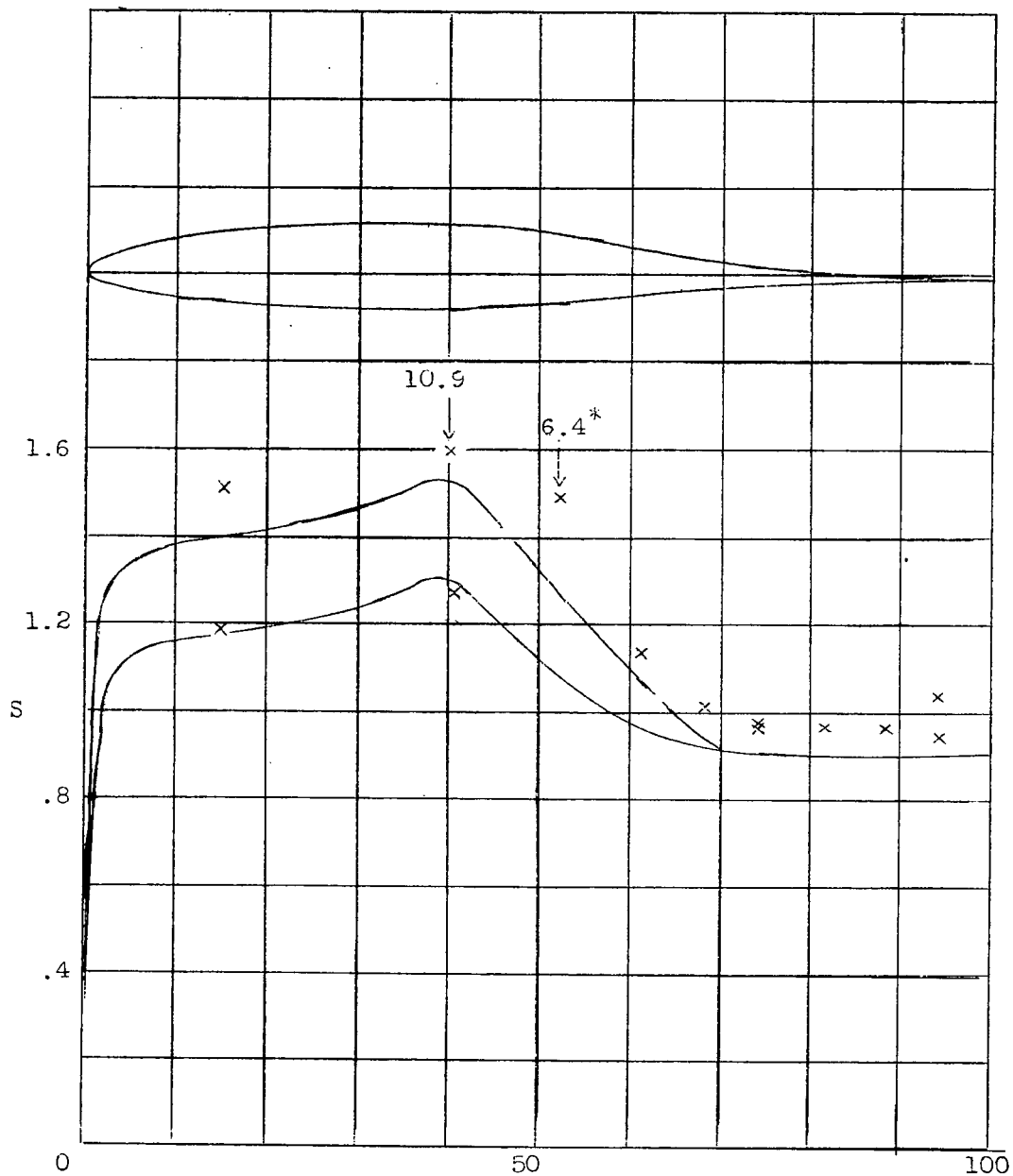


Figure 20.- NACA 27-215 airfoil.



	$\alpha$	$C_L$	$M_C$	$C_{d_{min}}$
Theory	$0^\circ$	0.133	0.71	-
Experiment	$1/2^\circ$	-	.69	0.0049 at $R=8.0 \times 10^6$

Figure 21.- NACA 27-215 airfoil with .5c extension.

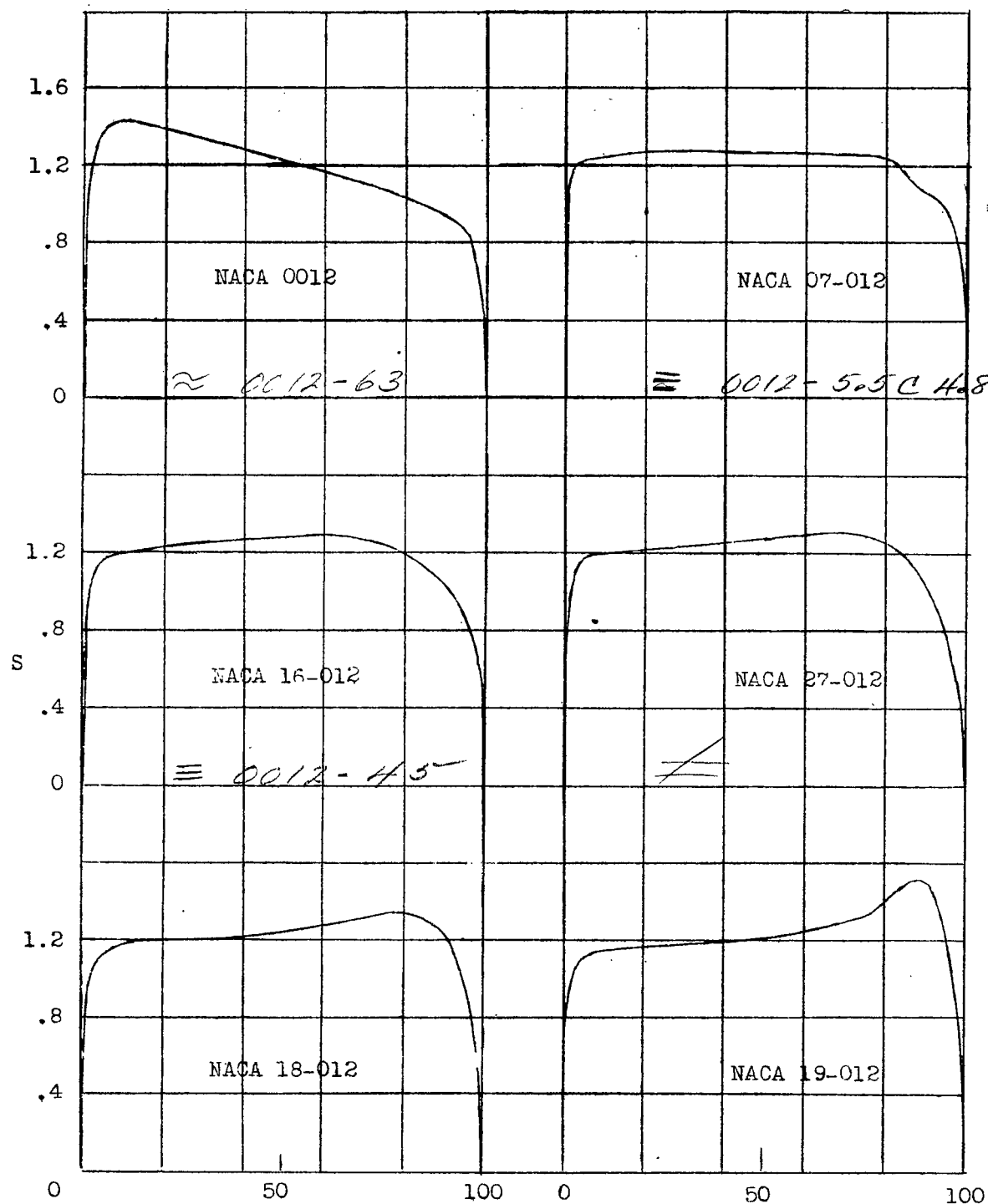


Figure 22.- Theoretical pressure distributions for the basic symmetrical sections.

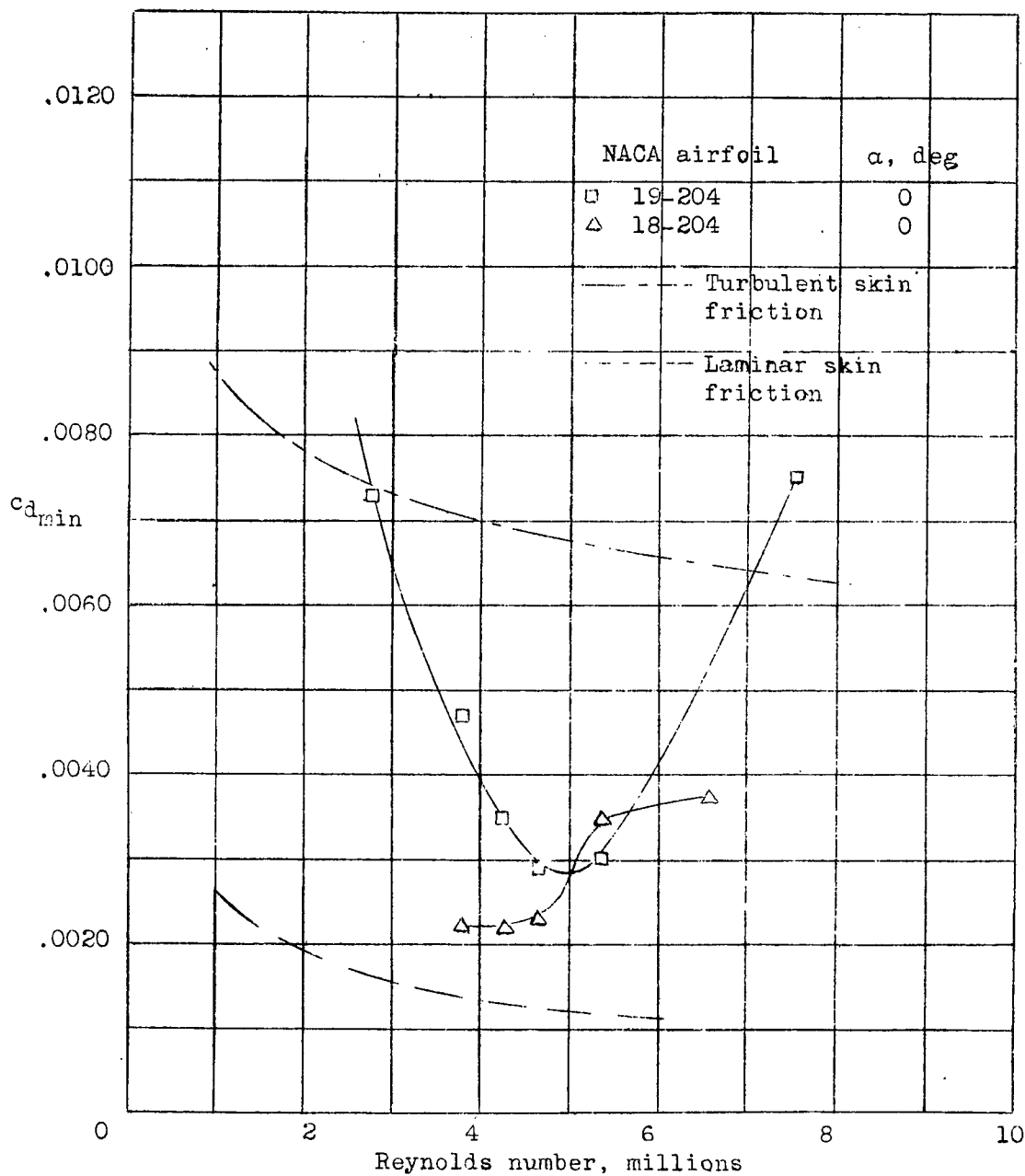


Figure 23.- Minimum drag coefficients of 4-percent-thick airfoils.

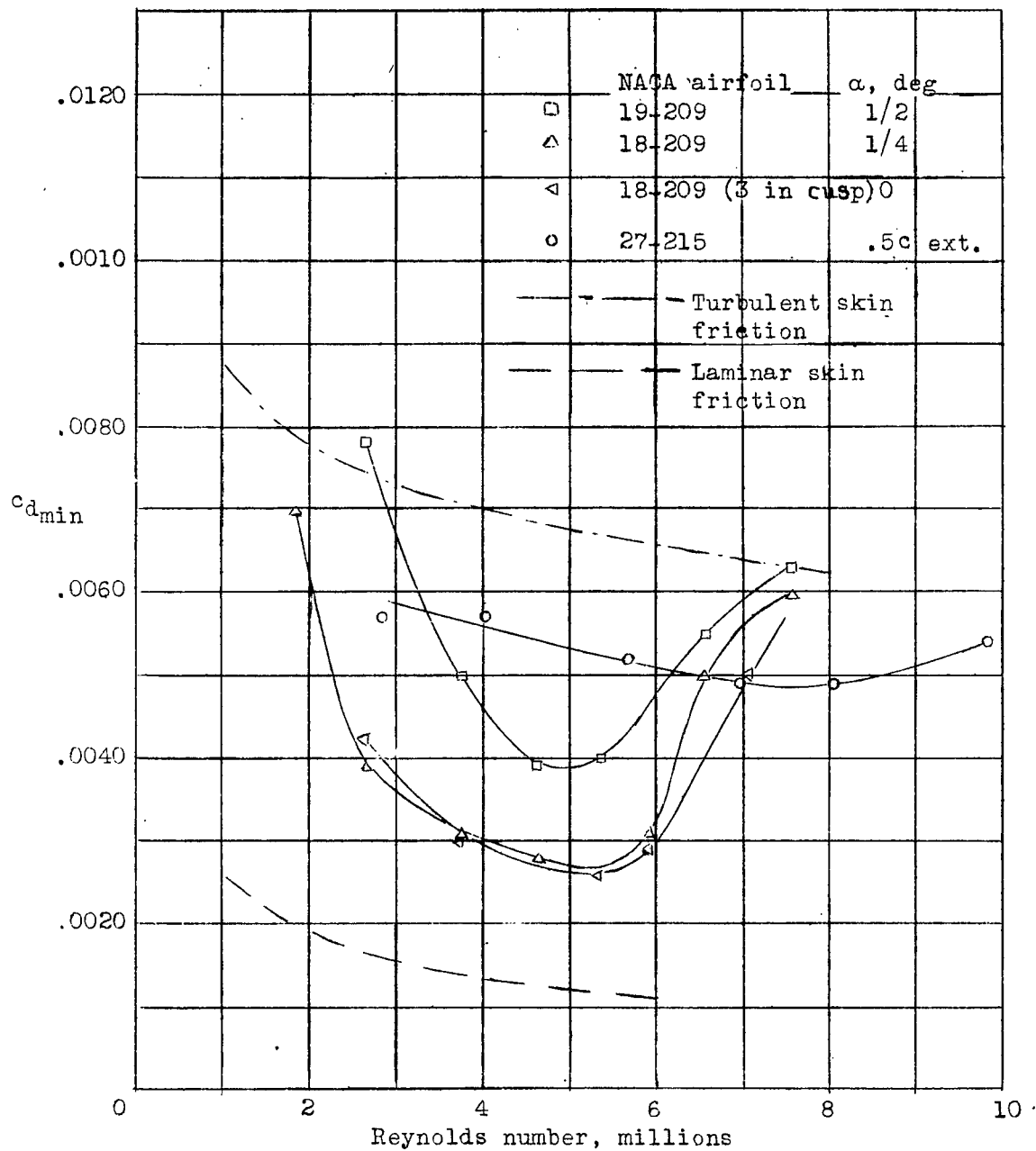


Figure 24.- Minimum drag coefficients.

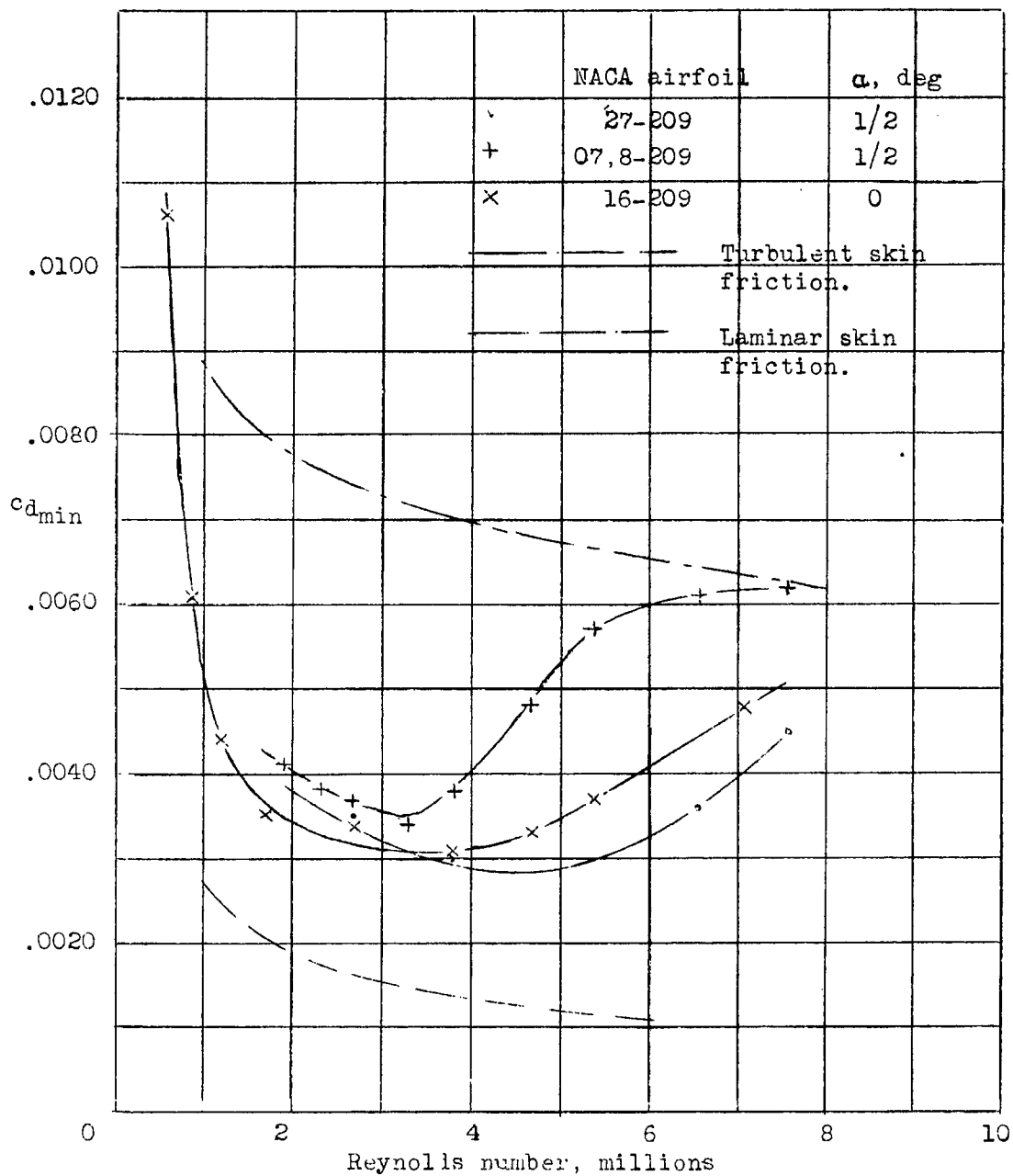


Figure 25.- Minimum drag coefficients  
of 9-percent-thick airfoils.

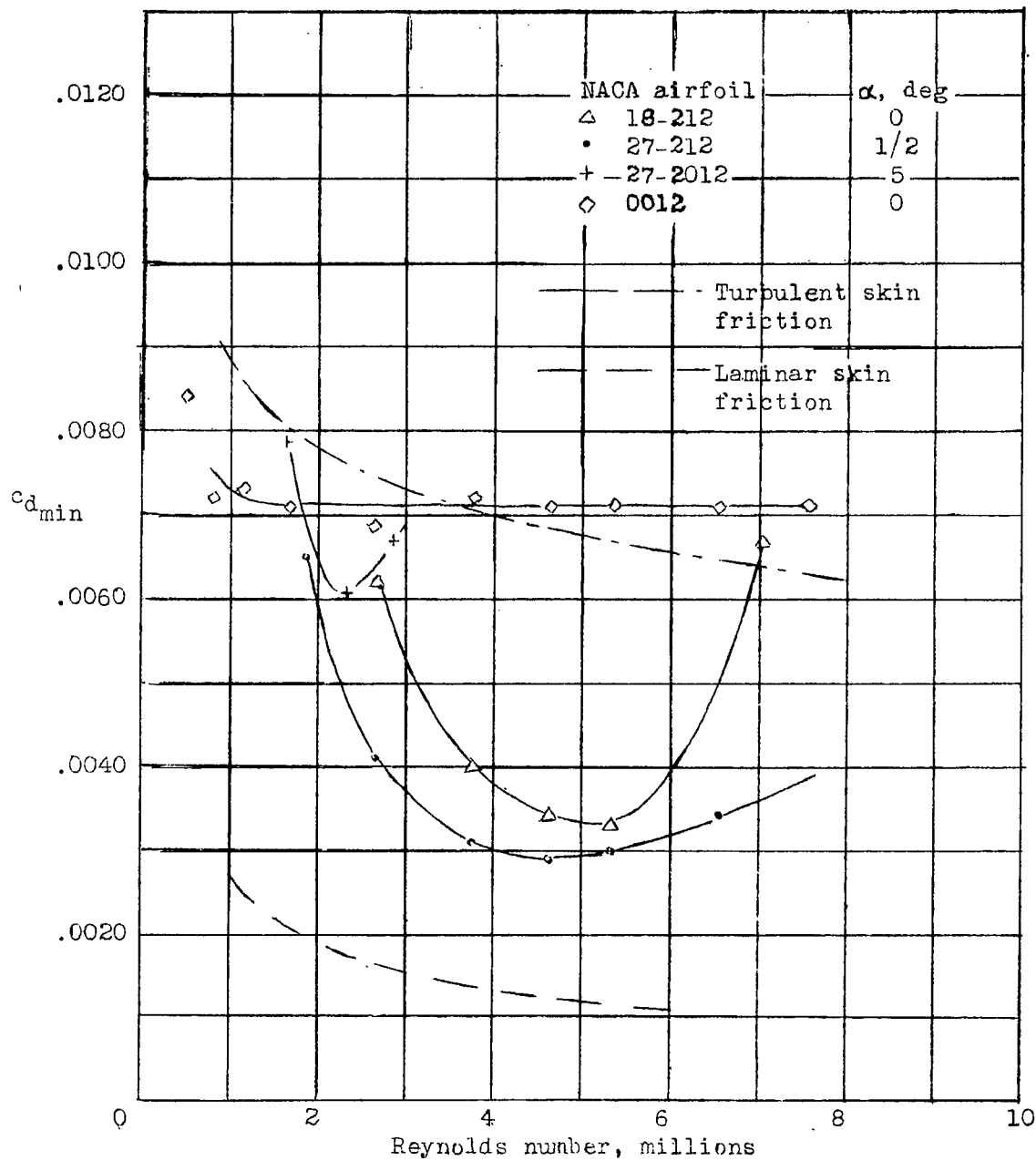


Figure 26.- Minimum drag coefficients of 12-percent-thick airfoils.

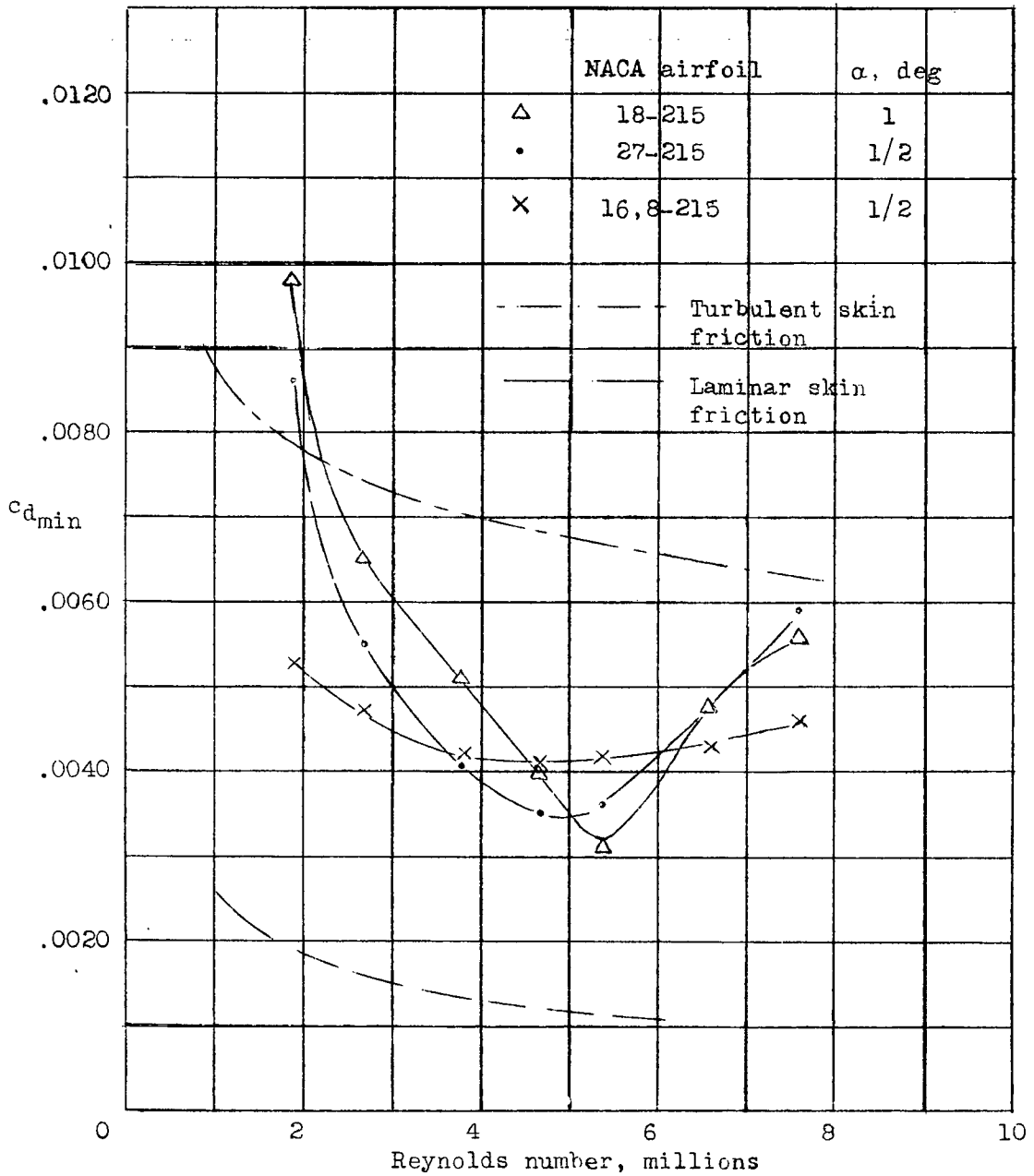


Figure 27.- Minimum drag coefficients of 15-percent-thick airfoils.

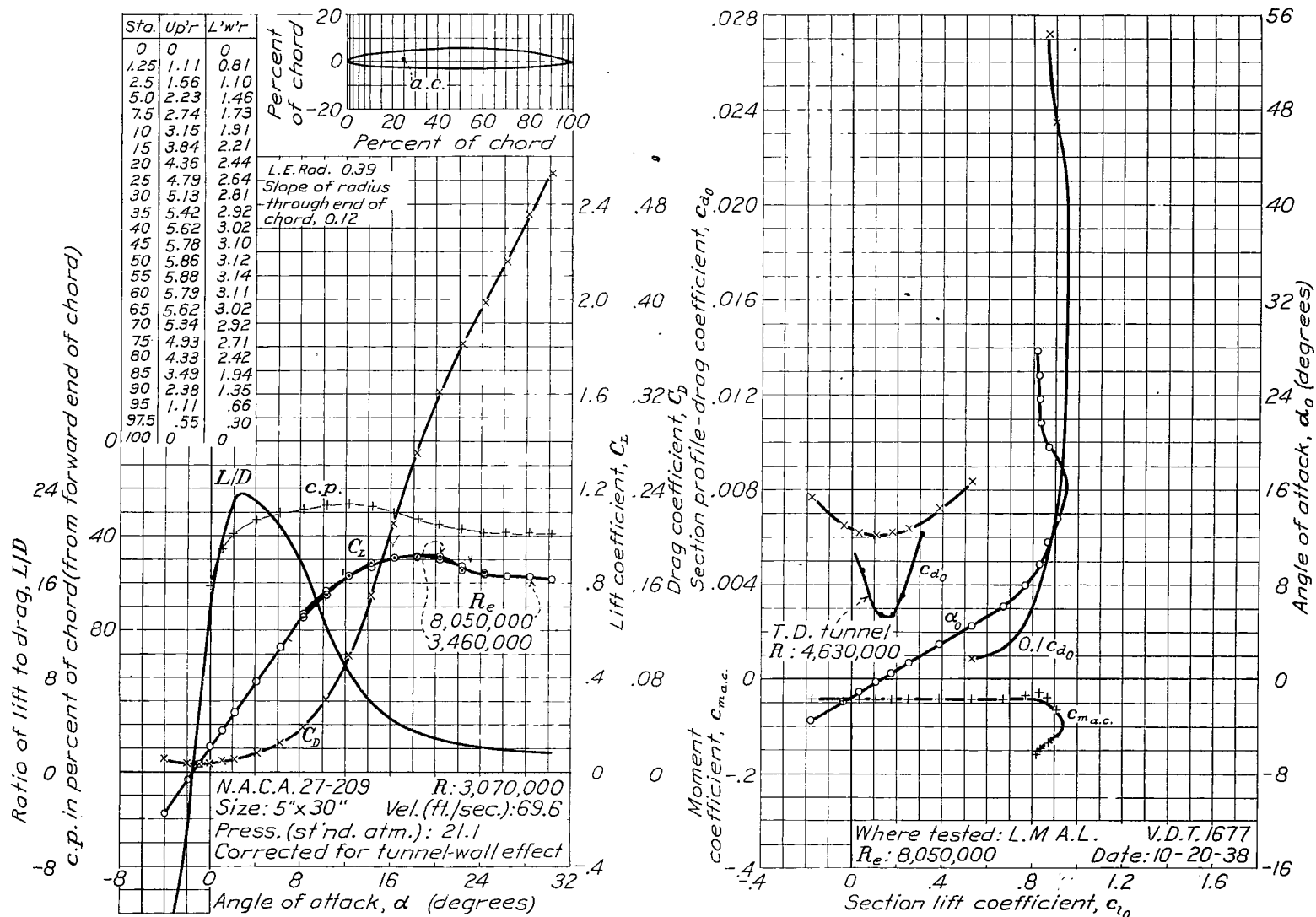


Figure 28

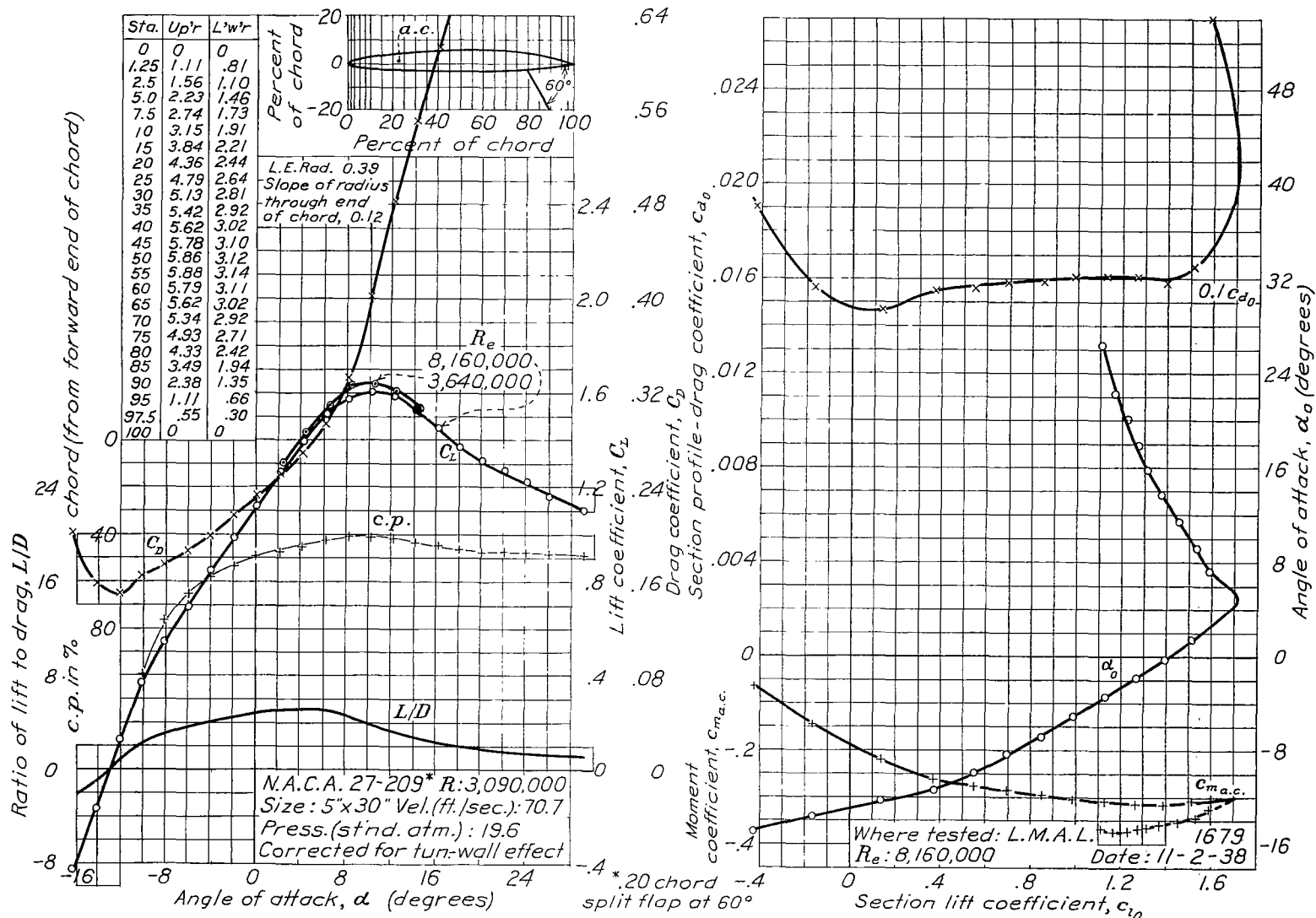


Figure 29

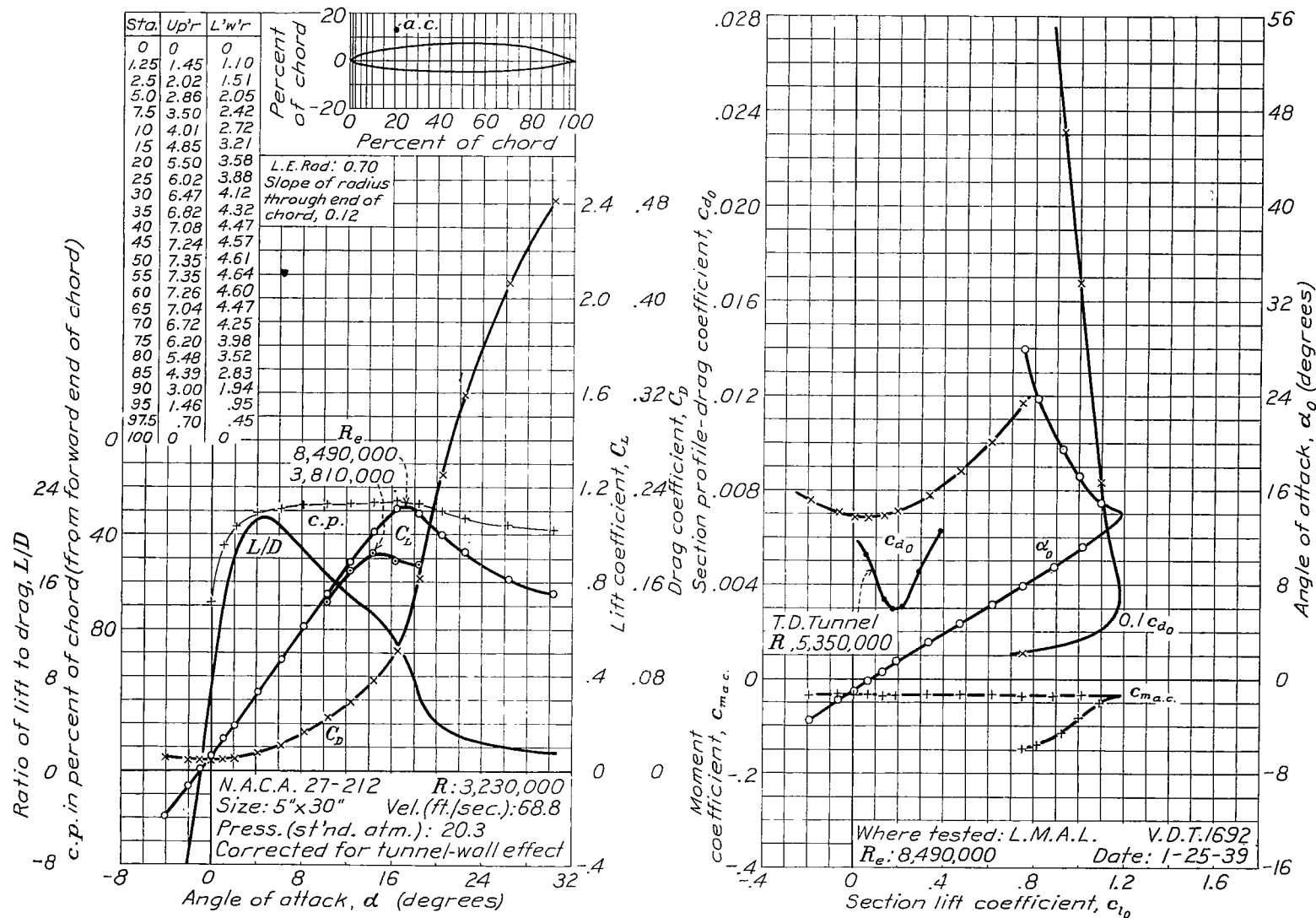
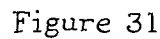


Figure 30



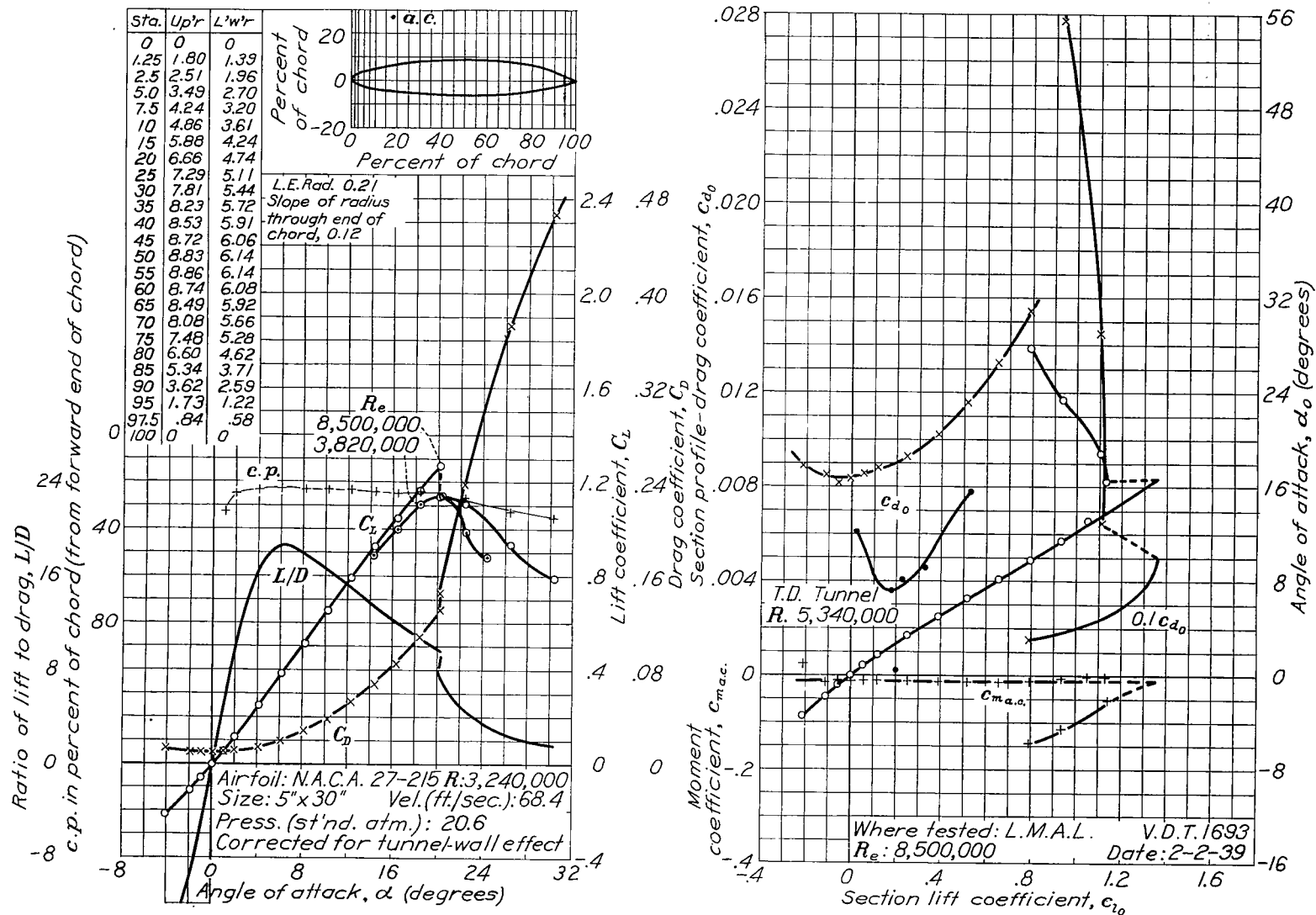


Figure 32

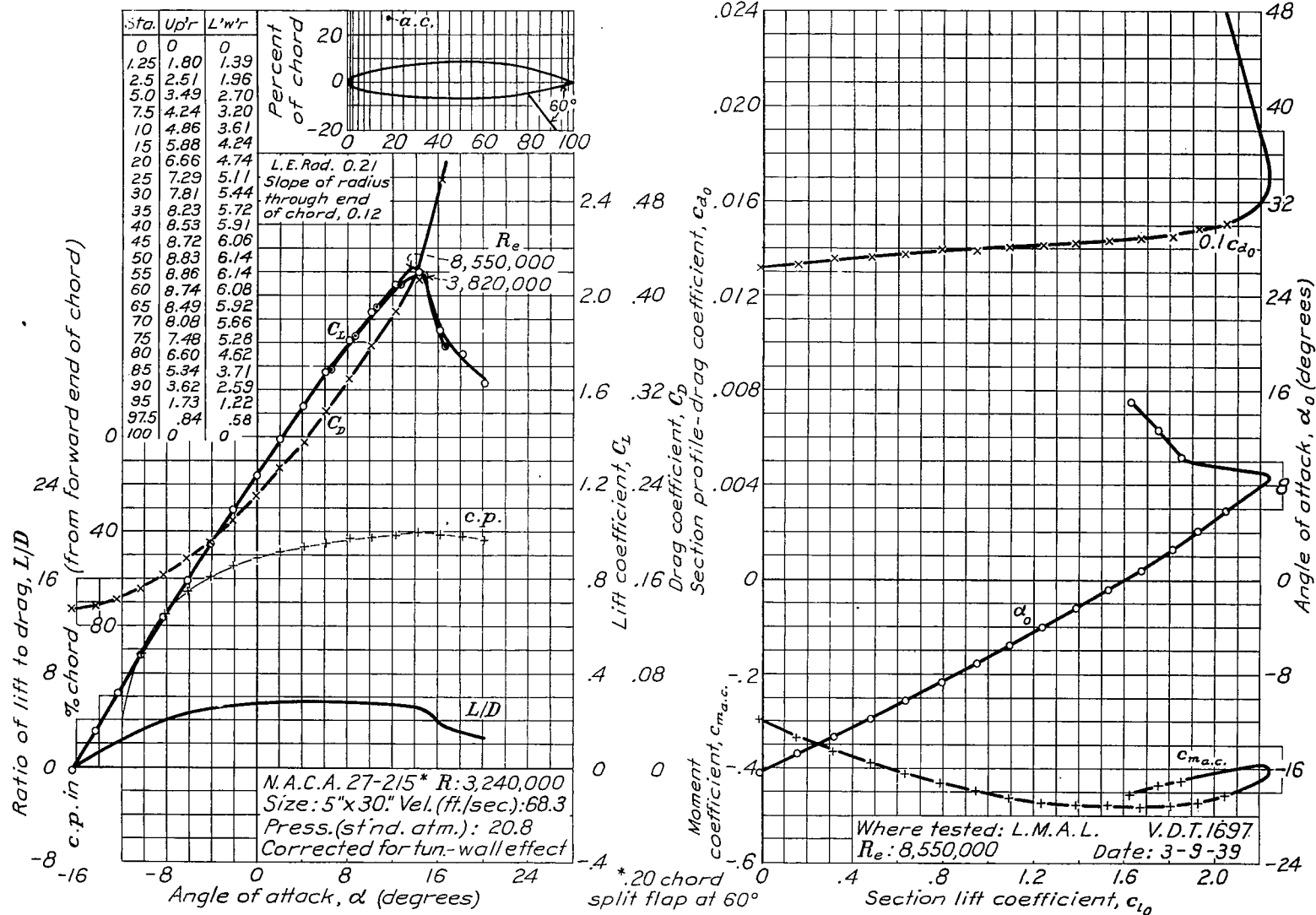


Figure 33